

Synthesis and Characterization of Multiphase, Highly Branched Polymers

Ann R. Fornof

Dissertation submitted to the faculty of the
Virginia Polytechnic Institute and State University
in partial fulfillment of the requirements for the degree of

Doctor of Philosophy
In
Macromolecular Science and Engineering

Timothy E. Long, Chair
Don Leo, Member
James McGrath, Member
Judy Riffle, Member
Thomas Ward, Member
Garth Wilkes, Member

April 20, 2006
Blacksburg, Virginia

Keywords: Highly Branched, Polyurethane, Ionene, Ionic Conductivity, Rheology,
Degree of Branching

Copyright 2006, Ann R. Fornof

Synthesis and Characterization of Multiphase, Highly Branched Polymers

Ann R. Fornof

ABSTRACT

Rheological modification is frequently cited as a key application for hyperbranched polymers. However, the high degree of branching in these polymers restricts entanglement and the resultant mechanical properties suffer. Longer distances between branch points may allow entanglements. Highly branched polymers, where linear units are incorporated between branch points, are synthesized with an *oligomeric* A_2 plus a monomeric B_3 . Highly branched polymers differ from traditional hyperbranched polymers in that every monomeric repeating unit of a hyperbranched polymer is a potential branch point, which is not true for highly branched polymers.

The *oligomeric* A_2 plus B_3 synthetic methodology was used for the synthesis of highly branched ionenes and polyurethanes. Highly branched ionenes, which have a quaternary ammonium salt in the main chain, were synthesized with a modified Menshutkin reaction. The *oligomeric* A_2 was comprised of well-defined telechelic tertiary amine endcapped poly(tetramethylene oxide). Reduced mechanical properties were observed for highly branched polymers compared to linear counterparts.

Highly branched polyurethanes were synthesized with polyether soft segments including poly(ethylene glycol), poly(tetramethylene glycol), and poly(propylene glycol). Degree of branching was determined via a novel ^{13}C NMR spectroscopy approach, which

is described herein. The classical degree of branching was supplemented with an alternative degree of branching equation, which was tailored for highly branched architectures. The melt and solution viscosities of highly branched poly(ether urethane)s were orders of magnitude lower than the linear analogs. For the first time, the presence of entanglements was confirmed for highly branched polymers. Doping the highly branched polyurethane with lithium perchlorate, a metal salt, resulted in a significantly higher melt viscosity. The ionic conductivity of the highly branched polyurethane when doped with a metal salt was orders of magnitude higher than the linear analog.

Soybean oil was oxidized for synthesis of soy-based polyol monomers. Three regimes were determined, and for the first time, a correlation between hydroxyl number and a resonance from the double bonds of soybean oil in ^1H NMR spectroscopy was described. The relationship was used to accurately describe oxidation of soybean oil with time, temperature, and air flow rate. Soybean oil oxidation was catalyzed, and tack-free films were formed.

ACKNOWLEDGEMENTS

I would like to thank my advisor, Prof. Timothy E. Long, for his guidance and invaluable advice throughout my graduate career. He has truly helped me appreciate “pushing back the frontiers of polymer science”. My committee members also significantly influenced the direction of my research. And I thank my committee members for their advice and help: Prof. Garth Wilkes, Prof. Tom Ward, Prof. Jim McGrath, Prof. Judy Riffle, and Prof. Don Leo. Thanks also to all of the staff, who have made my time in graduate school go more smoothly and enjoyably: Millie Ryan, Laurie Good, and Gary Scott. I also acknowledge the funding sources for my research: the Urethane Soy Systems Company, the MAP MURI, and the MS & IE IGERT. The opportunity to work with scientists from a variety of backgrounds was immeasurably helpful and interesting.

I would also like to thank all of my cohorts from Davidson 124a. Thanks to AJ Pasquale for having so much fun with me and for not letting me take myself too seriously. I would also like to thank Dr. Pasquale for his editing help, as well. I greatly appreciated Jeremy Lizotte’s friendship and mentorship while we were in the lab together. I don’t think that anyone has made me laugh quite so much while learning about science (and lifting weights), and I doubt I would have made it through my first year in graduate school without Jeremy’s influence and care. Scott Trenor for his mischievous adventures kept things lively in the lab. I would like to thank the other half of the dynamic duo, Matt McKee, for his willingness to indulge my rants about science and life. I appreciate greatly Matt’s patience and understanding in the lab. I would like to thank the more recent additions to Davidson 124a. Matthew Cashion was always willing to joke with (or

about) me. While it was difficult to hear myself think over John's heavy breathing and loud clock, John's wacky humor always made being in the lab an adventure. Rebecca Huyck was the first graduate woman to join me in Davidson 124a, and I greatly appreciate her friendship. The last few months would have been significantly more painful and less fun without her warmth in the lab. Thanks to Erika Borgerding for her help on these last few experiments. I am sure that she will carry on the tradition of great graduate students from Davidson. I also appreciate the help from the undergraduates, Matt and Allison, who worked with me in the lab over the years.

Thanks also to the other students and postdocs from the Long labs: Dave Williamson, Lars Kilian, Casey Elkins, Serkan Unal, Andy Duncan, Matt Hunley, Taigyoo Park, Sharlene Williams, Tomonori Saito, Amanda Willis, Gozde Ozturk, Qin Lin and Emily Anderson. Thanks to Brian Mather for his scientific advice and warm approach. The camaraderie of Afia Karikari and Kalpana Viswanathan has been a great bonus to graduating this year. I am glad that we were able to travel to conferences together and that we will experience graduation together. I greatly appreciate Dr. Cheryl Heisey's input on my writing. I would like to thank those people whose encouragement led me to pursue a doctorate degree: Dr. Jeff Hedrick, Prof. Chris Durning, Prof. Jeff Koberstein, and especially Dr. Christy Tyberg.

Thanks to all of my friends outside of the labs. The tailgating and happy hour crew provided some of the best times that I had in graduate school. Thanks to you all: DK, Doug, Josh, Som, Oak, Emmett, Lee, Sita, Chris, and Ben. Thanks especially to Mary for

all of the delicious food and your deliciously devilish sense of humor. I would like to thank the ultimate teams: Cleats and Cleavage and Jimmy Bang. Thanks for letting me join your ultimate family. Thanks especially to Lindsay and Corinne. Corinne, thank you for teaching me about ultimate, finally realizing how awesome I am, and letting me talk about my research. Lindsay has a fantastic perspective on life. She has the ability to make anyone around her feel special.

My family has been tremendously supportive during this sometimes tumultuous past few years. Thanks to my sister, Sarah Lewis, and my brother-in-law, Larry Lewis, for their love and support. I would like to express my deepest thanks to my parents, John and Judy Fornof. Their unconditional love and consideration during this process was tremendous. Thanks to my aunts and uncles, who despite their undying devotion to the Buckeyes, celebrated Hokie victories with me anyway.

I cannot imagine a better partner in life than my boyfriend, Mike Boylan-Kolchin. He has helped me to be a better person. On a number of levels, I would not be looking forward to getting our license plate “PhDz” without his love and encouragement.

Table of Contents

Chapter 1: Introduction.....	1
1.1 Dissertation Overview	1
Chapter 2: Review of the Literature.....	3
2.1 Introduction to Common Synthetic Routes	6
2.2 Degree of Branching Characterization.....	9
2.2.1 Degree of Branching Calculations.....	9
2.2.2 Degradation of Hyperbranched Polymers for Degree of Branching Determination	11
2.2.3 Indirect Methods for the Determination of the Degree of Branching.....	15
2.2.4 Enhancement of the Degree of Branching	16
2.3 Molecular Weight Characterization of Hyperbranched Polymers.....	18
2.3.1 Characterization of Hyperbranched Polymers with Size Exclusion Chromatography	18
2.3.2 Characterization of Hyperbranched Polymers with Matrix Assisted Laser Desorption/Ionization-Time of Flight Mass Spectrometry (MALDI-TOF/MS)	21
2.4 Rheological Behavior of Hyperbranched Polymers	22
2.4.1 Melt Rheology of Hyperbranched Polymers	23
2.4.2 Solution Rheological Behavior of Hyperbranched Polymers.....	32
2.5 Thermal Properties of Hyperbranched Polymers.....	34
2.5.1 Influence of Endgroups on Glass Transition of Hyperbranched Polymers	34
2.5.2 Thermal Stability of Hyperbranched Polymers	38
2.5.3 Impact of Hyperbranched Topology on Crystallization	39
2.6 References.....	41
Chapter 3: Synthesis and Characterization of Highly Branched Ioneners Containing Poly(tetramethylene oxide).....	49
3.1 Abstract.....	49
3.2 Introduction.....	51
3.3 Experimental.....	53
3.3.1 Materials	53
3.3.2 Synthesis of telechelic bis(dimethylamino) poly(tetramethylene oxide).....	53
3.3.3 Synthesis of highly branched ionenes.....	54
3.3.4 Synthesis of linear ionenes.....	55
3.3.5 Characterization	55
3.3 Results and Discussion	56
3.4 Conclusions.....	69
3.5 Acknowledgements.....	70
3.6 References.....	70
Chapter 4: Degree of Branching of Highly Branched Polyurethanes Synthesized via the <i>Oligomeric A₂ Plus B₃ Methodology: ¹³C NMR Spectroscopic Investigations</i>	73
4.1 Abstract.....	73
4.2 Introduction.....	74
4.3 Experimental.....	76
4.3.1 Materials	76

4.3.2 Synthesis of model compounds	77
4.3.3 Synthesis of linear polyurethanes	77
4.3.4 Synthesis of highly branched polyurethanes.....	77
4.3.5 Derivatization of endgroups.....	78
4.3.6 Polymer characterization	78
4.4 Results and Discussion	79
4.5 Conclusions.....	96
4.6 Acknowledgements.....	96
4.7 References.....	97
Chapter 5: Rheological Behavior and Ionic Conductivity of Highly Branched Poly(ether urethane)s for Electromechanical Devices.....	100
5.1 Abstract.....	100
5.2 Introduction.....	101
5.3 Experimental.....	103
5.3.1 Materials	103
5.3.2 Synthesis of linear polyurethanes	104
5.3.3 Synthesis of highly branched polyurethanes.....	104
5.3.4 Addition of salt to polyurethane	105
5.3.5 Polymer Characterization.....	105
5.4 Results and Discussion	106
5.5 Conclusions.....	125
5.6 Acknowledgements.....	126
5.7 References.....	126
Chapter 6: Synthesis and Characterization of Triglyceride-Based Polyols and Tack-Free Coatings via the Air Oxidation of Soy Oil.....	132
6.1 Abstract.....	132
6.2 Introduction.....	133
6.3 Experimental.....	136
6.3.1 Statistical Design of Experiments.....	136
6.3.2 Air Oxidation	136
6.3.3 Hydroxyl Number Determination	137
6.3.4 Film Formation	138
6.4 Results and Discussion	139
6.4.1 High molecular weight polyols.....	139
6.4.2 Crosslinked coatings	148
6.5 Conclusions.....	153
6.6 Acknowledgements.....	154
6.7 References.....	154
Chapter 7: Overall Conclusions	158
Chapter 8: Suggested Future Work.....	161
8.1 Synthesis and Gene Transfection Studies of PEG-Based Ionenenes.....	161
8.2 Highly Branched PTMO-Based Ionenenes with Viologen-Type Branching Agents.....	161
8.3 Ionic Conductivity of Highly Branched, PTMO-Based Ionenenes.....	162
8.4 Probe the Influence of Hard Segment on Ionic Conductivity and Interaction with Lithium Salts.....	163

8.5 Determine the Influence of Branching on the Swelling Behavior of PEG-based Polyurethanes	164
8.6 Determine Influence of Hydrogen Bonding on Melt Rheological Behavior	164
Appendices	166
Vita.....	170

List of Figures

Figure 2.1: Depiction of differences between A_2 plus B_3 polymerization and hyperbranched polymers from AB_2 monomers ²⁹	7
Figure 2.2: First steps of SCVP polymerization ⁵⁴	8
Figure 2.3: DB and fraction of branch points with conversion for SCVP hyperbranched polymers and AB_2 hyperbranched polymers ⁵⁴	11
Figure 2.4: Endcapping and degradation of an aryl polyester for degree of branching analysis ⁶⁹	14
Figure 2.5: DB versus conversion for different steps of monomer addition a) simultaneous addition of A_2 and B_3 , b) addition of B_3 to a solution of A_2 ⁷⁴	17
Figure 2.6: Variation of Mark-Houwink exponent with increasing spacer segment length in hyperbranched polyethers ⁷⁸	19
Figure 2.7: Number average degree of polymerization and polydispersity vs. conversion, where the solid lines are theoretical predictions ⁷⁹	20
Figure 2.8: Universal scaling plot, where τ is approximately 1.53 ⁸²	21
Figure 2.9: Weaker scaling of η_0 with M_w of hyperbranched polystyrene compared to linear polystyrene ⁸⁸	24
Figure 2.10: Relationship between η_0 and M_w for hyperbranched polyesters ⁸⁹	25
Figure 2.11: Good fit of Rouse-based dynamic scaling model to loss and storage modulus from hyperbranched polyesters indicating that the polyesters were unentangled ⁹	27
Figure 2.12: Temperature dependence of viscosity for hyperbranched poly(ϵ -caprolactone)s ⁹⁷	28
Figure 2.13: Illustration of hyperbranched polymer with a large number of terminal, B, groups ³³	29
Figure 2.14: Influence of temperature on viscosity of hyperbranched polyesters with increasing molecular weight from sample H20 (2,100 g/mol) to H50 (7,500 g/mol) ⁹³	30
Figure 2.15: Non-terminal scaling of hyperbranched poly(ϵ -caprolactone)s ⁹⁶	31
Figure 2.16: Influence of the increasing length of alkyl endcapper, which reduced the hydrogen bonding capability, on Tg of an aromatic hyperbranched polyester ⁶⁸	36
Figure 2.17: Reduction in Tg with replacement of hydroxyl, hydrogen bonding, endgroups with alkyl, non-polar, endgroups ¹¹⁸	37
Figure 2.18: Good thermal stability of two hyperbranched fluoropolymers ¹²¹	39
Figure 2.19: Influence of the degree of branching on the relative degree of crystallinity and the influence of dendritic, linear, and terminal units on the relative degree of crystallinity ¹²⁹	40
Figure 3.1: Dynamic mechanical analysis of highly branched and linear ionenes based on 2,000 and 7,000 g/mol PTMO	60
Figure 3.2: TGA of linear and highly branched ionenes	63
Figure 3.3: Melt rheological behavior of linear and highly branched ionenes. LI-7k and LI-2k overlap in both plots. a) storage modulus versus frequency b) complex viscosity versus frequency at 80 °C	66
Figure 3.4: Tensile behavior of linear and highly branched ionenes at 25 °C. Inset: comparison of highly branched polymers	68

Figure 4.1: Resonances from ^{13}C NMR spectroscopy of model compounds derived from cyclohexyl isocyanate compared with the polyurethane a.) methyl region, b.) methylene region, c.) carbonyl region, d.) quaternary carbon region	83
Figure 4.2: Quaternary carbon region of the ^{13}C NMR of the phenyl isocyanate-based model compounds and mass spectroscopy data.....	85
Figure 4.3: Quantitative ^{13}C NMR spectrum of the highly branched polyurethane.....	87
Figure 4.4: Quantitative ^{13}C NMR spectrum of the trifluoroester endcapped highly branched polyurethane.....	87
Figure 4.5: Edited ^{13}C DEPT NMR spectrum indicating the presence of quaternary carbons in the 45-40 ppm region of the ^{13}C NMR spectrum of the highly branched polyurethanes	89
Figure 4.6: SEC chromatograms for increasing addition of A ₂	91
However, previous efforts with the <i>oligomeric</i> A ₂ plus B ₃ synthetic strategy revealed expected degrees of branching. ¹⁷³	91
Figure 4.7: Intrinsic viscosity across the molecular weight distribution for two PEG-based, highly branched polyurethanes (□, 2,000 g/mol PEG; *, 600 g/mol PEG).....	92
Figure 4.8: Trend of decreasing DB (%) as calculated by equation (4) with increasing molecular weight of the oligomeric A ₂ group.....	95
Figure 4.9: Impedance plane plot of highly branched polyurethane doped with 8:1 lithium perchlorate.....	95
Figure 5.1: Lower complex viscosity of highly branched oligomeric A ₂ plus B ₃ compared with linear analog.....	109
Figure 5.2: Dependence of η_0 on Mw for a highly branched polyurethane series. The η_0 —M _w relationship is similar to the 3.4 theoretical prediction for linear polymers.	111
Figure 5.3: Systematic decrease in melt viscosity with increase degree of branching ...	113
Figure 5.4: Exponential dependence of (a) zero shear rate viscosity and (b) longest relaxation time on the contraction factor, g' . Significant (R ² = 1) relationship (c) between the contraction factor, g' , and DB ²	115
Figure 5.5: Dynamic moduli of highly branched polyurethanes with DB ₂ of 6.2% (squares) and 8.0% (circles). Intersection of G' (open symbols) and G'' (closed symbols) is related to the relaxation time.	116
Figure 5.6: Master plot of storage modulus of a highly branched polyurethane at T _{ref} = 80 °C Lack of a plateau in the storage modulus of highly branched polyurethanes was attributed to the high 2.51 polydispersity.	119
Figure 5.7: Comparison of the specific viscosity for a linear and highly branched polyurethane of equal hard segment content (57%), soft segment composition (600 g/mol PEG), and molecular weight (40,000 g/mol) over a wide concentration range in DMF. The intersection of the semi-dilute unentangled and semi-dilute entangled regime indicates the entanglement concentrations. The slopes of the semi-dilute unentangled regime for both polymers were 1.78 and 3.1 and 3.5 for the semi-dilute entangled concentration regime for the highly branched and linear polymers, respectively.	120
Figure 5.8: Melt rheology of linear and highly branched (HB) polyurethanes with 8:1 ethylene oxide : lithium perchlorate doping level. a) melt complex viscosity at T _{ref} = 80 oC b) dynamic modulus data	123
Figure 5.9: Ionic conductivity for PEG 600 g/mol-based polyurethane.....	124
Figure 6.1. Isothermal TGA of raw soybean oil at 150 °C under oxygen.....	142

Figure 6.2. 3-D plots of temperature and time dependence of first regime of oxidation for normalized doubly allylic resonance integration and hydroxyl number.....	143
Figure 6.3. Significant relationship between the normalized integration of the doubly allylic resonance and hydroxyl number.....	144
Figure 6.4. Decrease in normalized doubly allylic resonance from ¹ H NMR spectra indicating an increase in hydroxyl number of soy polyols.....	146
Figure 6.5. Increase in viscosity observed with time at 100 °C, 25 L/min. Raw soybean oil and 1 day are superimposable at the lowest viscosity.....	147
Figure 6.6: Effect of pressure on soybean oil oxidation at 110 °C for one day.....	148
Figure 6.7: Change in normalized doubly allylic resonance with time at 110 oC under 75 psi charged air pressure.....	149
Figure 6.8. Decrease in tack of films over time at elevated temperatures.....	150
Figure 6.9. Percent gel of soybean oil coatings.....	151
Figure 6.10. Decrease in tack observed with increasing UV irradiation for coatings cured at 100 °C for 60 min.....	152
Figure 6.11. Increase in absorbance at 240 nm observed with an increase in hydroxyl number.....	153

List of Tables

Table 3.1: Summary of DSC data from highly branched and linear ionenes	59
Table 3.2: Mechanical properties of linear and highly branched ionenes	69
Table 4.1: Degree of branching results highly branched poly(ether urethane)s	90
Table 4.2: Influence of increasing addition of A2 from 2,000 g/mol PTMO on degree of branching for highly branched polyurethanes.....	94
Table 5.1: Increasing ratio of A2 : B3 led to increased molecular weight and zero shear rate viscosity.	110
Table 5.2: Influence of branching in polyurethanes on rheological behavior.	112
Table 5.3: Influence of higher hard segment content on zero shear rate viscosity	117
Table 6.1. Molecular weight and hydroxyl number data for soybean oil oxidized at 110 °C	145

List of Schemes

Scheme 3.1: Synthesis of BAPTMO, <i>oligomeric A₂</i>	57
Scheme 3.2: Highly branched ionene synthetic scheme.....	58
Scheme 4.1: Synthesis of highly branched polyurethanes with TMP B3 branching agent	80
Scheme 4.2: Synthesis of model compounds.....	82
Scheme 6.1. Air oxidation of triglyceride yields hydroxyl groups replacing allylic protons.....	140
Scheme 8.1 Synthetic scheme for viologen-type, highly branched, PTMO-based ionenes	162

Chapter 1: Introduction

1.1 Dissertation Overview

Polymer topology is a primary tool for adjusting the physical properties and functionality of polymers. Branching influences the processability and the applications of polymers. Hyperbranched polymers, where every monomer unit is a potential branch point, has received significant interest in the literature due to the globular structure, high functionality, and which lends itself to creative approaches to synthesis. The commercial availability and the symmetry of the monomers used in the A_2 plus B_3 synthetic approach to hyperbranched polymers are advantages when compared with the traditional polycondensation of AB_x -type monomers. Recently, the polymerization of oligomeric A_2 plus B_3 was proposed. The goal of this approach was to provide distances between branch points, which are long enough for entanglements.

The synergy between a high degree of branching and intermolecular interactions was investigated in this dissertation. Following this chapter, characterization techniques used for hyperbranched polymers were reviewed. The third chapter deals with systematic branching of ionenes. The effect of branching in the hard segment on the intermolecular interactions and mechanical properties was addressed. In the fourth chapter, highly branched PEG-based polyurethanes were synthesized. The degree of branching was determined with a novel ^{13}C NMR spectroscopy approach. An alternative degree of branching calculation was also proposed. The fifth chapter describes the reduced melt and solution viscosities of highly branched polymers compared to linear analogs. The ionic conductivity of highly branched polyurethanes was improved over linear analogs.

The sixth chapter focused on the synthesis of monomers from renewable resources for potential use in microphase separated polymers. The seventh chapter summarizes the accomplishments of this dissertation work.

Chapter 2: Review of the Literature

The determination of the fundamental effects of branching on a variety of applications ranging from rheological modification to electrospinning has received intense scrutiny.^{1,2} Long chain branching increases the melt viscosity compared to linear analogs due to an increase in entanglements. However, short-chain branched polymers have fewer entanglements causing a reduction in melt and solution viscosities and hydrodynamic radius. Long-chain branching also has a significant affect on the shear thinning of sparsely branched polymers. With the incorporation of a small number of long-chain branched polymers, the onset of shear-thinning occurs at lower frequencies than for linear counterparts.^{1, 3} Numerous topologies were synthesized to probe the effects of branching from pom poms to star polymers. Dendrimers emerged as a novel, monodisperse, wholly branched topology. Dendritic polymers were interesting academically but the synthetic rigor required for dendrimers made them inaccessible for most industrial applications. Hyperbranched polymers emerged as an industrially viable, highly branched alternative to dendrimers. Unlike dendritic polymers, hyperbranched polymers have imperfections and are not wholly branched. Hyperbranched polymers are polydisperse with isomers and different geometries whereas dendrimers are monodisperse and have a single, well-defined architecture.

In the last fifteen years, a resurgence of interest in hyperbranched polymers has occurred. Flory's theoretical treatment of polymers synthesized with AB_x type monomers laid the groundwork for studies of hyperbranched polymers.^{4, 5} The properties of hyperbranched polymers, which include increased solubility, low viscosity, large numbers of chain ends for functionalization, make this polymer class potentially useful

industrially and academically interesting. The lower viscosity of hyperbranched polymers compared to linear counterparts has received significant attention.⁶⁻⁸ The globular shape of hyperbranched polymers and short distances between branch points prohibit entanglements.⁹ However, the exclusion of entanglements created polymers without significant mechanical properties. This led to the frequent citation of rheological modification as an industrial application for hyperbranched polymers.¹⁰⁻¹⁴ Recent work utilizing the synthetic strategy of an oligomeric A₂ plus B₃ monomer has introduced a high degree of branching with long linear segments for entanglements and improved mechanical properties compared with traditional hyperbranched polymers.^{1, 7, 15, 16}

Spectroscopic and chromatographic methods are frequently used for the characterization of long- and short-chain branching. Determination of branch points with ¹³C NMR spectroscopy is useful for branching concentrations greater than 10⁻⁴.¹⁷ Zimm and Stockmayer first proposed a contraction factor, *g*, for the description of long chain branching.¹⁸ The contraction factor, *g*, is defined as the ratio of the radii of gyration for the branched and linear polymers, $\langle R_g^2 \rangle_{br} / \langle R_g^2 \rangle_{lin}$. Dilute solution measurements, typically size exclusion chromatography (SEC) with light scattering, are frequently used to find the radius of gyration for the calculation of *g*. Light scattering has limitations for the determination of the radius of gyration at small or moderate radii. The ratio of the intrinsic viscosities of branched and linear polymers, *g'*, avoided the difficulties of light scattering and provided an avenue to determine an alternative contraction factor, where $g' = [\eta]_{br} / [\eta]_{lin}$.¹⁹ The relationship between the two contraction factors, $g' = g^\epsilon$, was based on the Fox-Flory equation, and it was suggested that $\epsilon = 3/2$.²⁰ Zimm and Kilb reconsidered the value of ϵ about 10 years after the first publication and determined that

$\epsilon = 1/2$.²¹ Considerable debate continues about the relationship between the contraction factors. It was suggested that a power law relationship alone cannot describe the relationship between g and g' .²²⁻²⁴ Spectroscopic and chromatographic methods including NMR, IR, and SEC lack the sensitivity to detect sparse long-chain branching, which has a substantial effect on rheological behavior.²⁵ Creative solutions to the problem of the characterization of long- and short-chain branched polymers have received sizeable effort. The sensitivity of dilute solution behavior that gives rise to the ratio g is insufficient to detect sparse long-chain branching that significantly affects melt rheological behavior.²⁶ Short-chain branching is frequently achieved through copolymerization. Therefore, the quantity of short-chain branching is typically identifiable through the amount of comonomer charged to the reaction. The distribution of short-chain branching, and its affect on mechanical properties has received considerable attention. The density and temperature rising elution fractionation are two techniques that indicate the amount and distribution of short-chain branching.²⁷

The task of characterizing long- and short-chain branching has produced several techniques that are useful in the characterization of different topologies including hyperbranched polymers. However, the highly branched nature of hyperbranched polymers creates its own challenges for characterization. The greater branching density presents opportunities for the characterization of hyperbranched polymers. This review addresses the unique behavior and characterization of hyperbranched polymers. A brief treatment of synthetic strategies is warranted to understand the basis for the characterizaiton. However, most reviews on the subject of hyperbranched polymers are devoted primarily to the synthetic considerations.²⁸⁻³³

2.1 Introduction to Common Synthetic Routes

The approaches to step-growth polymerization of hyperbranched polymers can be broken down into two primary synthetic strategies: 1.) those that use AB_x monomers and 2.) polymerizations based on A_2 and B_3 monomers. Synthesis of hyperbranched polymers via step growth polymerization is traditionally performed with AB_x monomers, where $x \geq 2$. The polycondensation of AB_x monomers is a one-pot synthesis, and it was theoretically determined that no gelation will ensue from this type of reaction.^{11, 34-39} One distinct disadvantage of AB_x -type polymerizations is the synthetic effort required for the synthesis of the AB_x monomers, which are frequently not commercially available. A variety of synthetic techniques and monomer chemistries were employed for the synthesis of hyperbranched polymers with AB_x monomers. The most common polymers synthesized from AB_x monomers include polyesters⁴⁰⁻⁴², polyphenylenes^{11, 43, 44}, and polyamides^{45, 46}. Several hyperbranched polyesters are commercially available, which is becoming more frequent but is still a distinction for hyperbranched polymers.^{47, 48}

Another common step-growth approach for the synthesis of hyperbranched polymers is the addition of A_2 plus B_3 monomers. The commercial availability of A_2 and B_3 monomers is a primary advantage of this synthetic route. Careful synthetic techniques are necessary to avoid gelation. Slow monomer addition, dilution, and exact stoichiometry are all techniques employed to avoid gelation. An illustration of the differences between AB_x and A_2 plus B_3 polymerizations is shown in Figure 2.1.

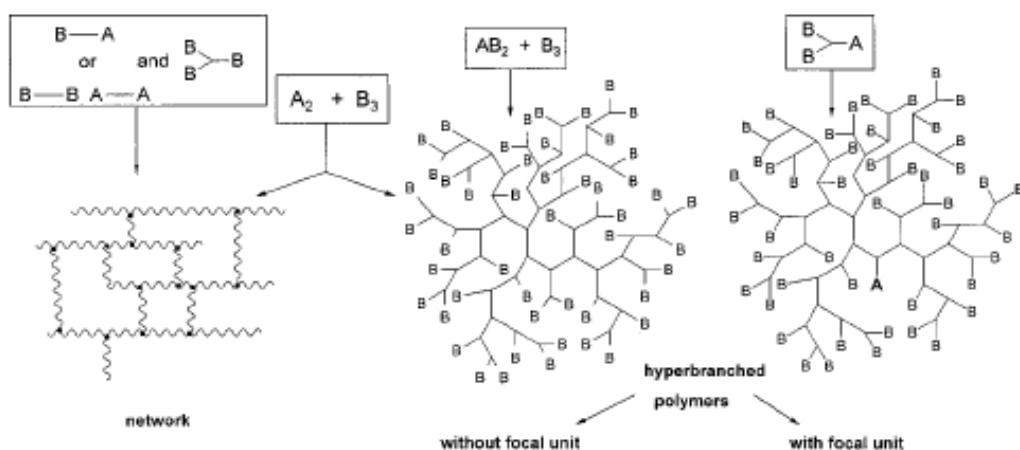


Figure 2.1: Depiction of differences between A_2 plus B_3 polymerization and hyperbranched polymers from AB_2 monomers²⁹

Self-condensing vinyl polymerization (SCVP) occurs with monomers containing one vinyl group, A, and one initiating group, B^* , (AB^* monomers). Hyperbranched polymers synthesized from SCVP typically rarely crosslink when living/controlled conditions are used. The polydispersity of SCVP hyperbranched polymers is theoretically much greater than that of hyperbranched polymers from AB_2 monomers.⁴⁹ Synthetic techniques for lower polydispersity hyperbranched polymers are frequently used.^{50, 51} Cations, radicals, and carbanions are all possibilities for the active center in SCVP.^{15, 52, 53} An example of an SCVP monomer and the first few steps are shown in Figure 2.2.

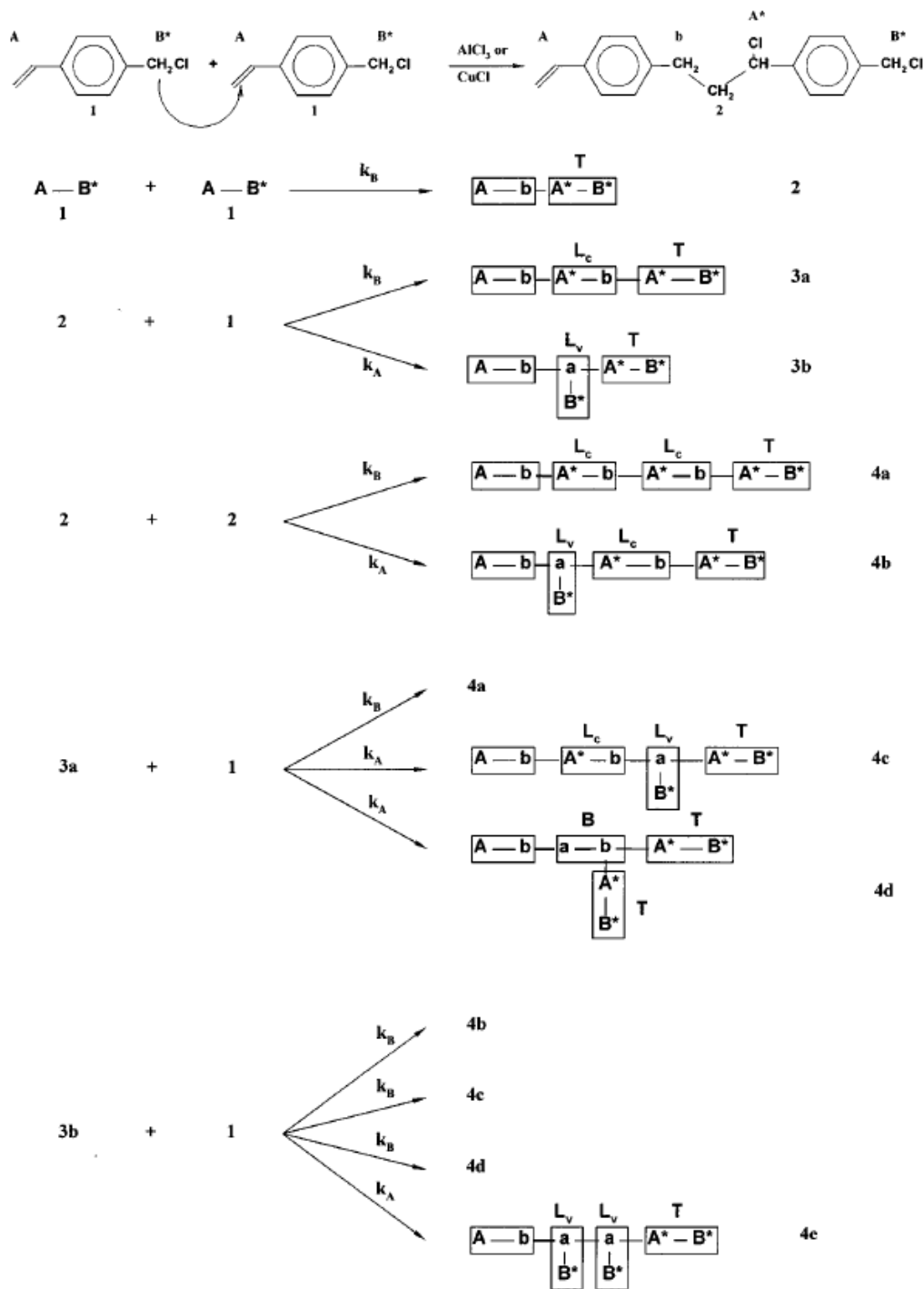


Figure 2.2: First steps of SCVP polymerization⁵⁴

2.2 Degree of Branching Characterization

While dendrimers are monodisperse and have a regular structure, hyperbranched polymers are polydisperse and have irregular dendritic structures, which include isomers and different geometrical shapes. The degree of perfection of the hyperbranched polymer was described with the degree of branching calculation. The degree of branching is one of the most important characterizations of a hyperbranched polymer in that it describes the branching efficiency.³²

2.2.1 Degree of Branching Calculations

Hawker et al. described a degree of branching equation to describe the irregular structures of hyperbranched polymers.³⁶ In this equation, three units are described: dendritic, D; linear, L; and terminal, T. The units that contribute to a wholly branched polymer are divided by all of the units in the hyperbranched polymer.

$$DB = (D + T)/(D + L + T) \quad (1)$$

A greater incorporation of linear units results in a decrease in the degree of branching. This equation is frequently utilized for the description of the degree of branching for hyperbranched polymers synthesized with AB₂ monomers.⁵⁵⁻⁵⁷ Kim et al. described a branching factor, f_{br} , which is similar to the degree of branching equation that Hawker et al. proposed, to replace the conventional degree of branching (α)⁵⁸ for hyperbranched polymers from AB₂ monomers.

$$f_{br} = (T+B)/N_0 \quad (2)$$

In this equation, the branching factor is equal to the sum of the mole fraction of terminal units to the mole fraction of the branched units, which was described as dendritic in the

previous equation, divided by N_0 . N_0 is the sum of the terminal, branched, and linear units of the hyperbranched polymer.^{32, 59}

Several years after the original degree of branching equations were proposed Hölder et al. sought to describe a DB equation for hyperbranched polymers that was accurate for low molecular weight hyperbranched polymers from AB_2 monomers. The following equation was proposed:

$$DB = 2D/(2D + L) \quad (3)$$

The results from the equation described by Hölder et al. are approximately the same as those from Eqn (1) for high molecular weight polymers. Frequently, DB is calculated from Eqns (1) and (3), and a comparison of the results is reported.⁶⁰⁻⁶² Hölder et al. also addressed DB for the general case of hyperbranched polymers from AB_m monomers, where $m \geq 2$. The DB for the random reaction, where the reactivity of A and B groups remains the same throughout the reaction, was described as:

$$DB = [(m-1)/m]*\exp(m-1) \quad (4)$$

It was found that at high values of m the DB approaches a value of 0.368.

A degree of branching was proposed to describe hyperbranched polymers from self-condensing vinyl polymerization (SCVP).⁵⁴ A schematic of the first steps of an SCVP polymerization is shown in Figure 2.2.

The incorporation of two linear units, L_c and L_v , made a new definition of a degree of branching for SCVP hyperbranched polymers useful. Prior to the introduction of the degree of branching calculation for hyperbranched polymers synthesized with SCVP, the

authors modified the degree of branching from eqn (1). Yan et al. proposed the following equation for the degree of branching calculation:

$$DB = 2B/(1-M-2A') \quad (5)$$

where B is the number of branched units; M is the residual amount of monomer; and A' is the fraction of vinyl groups attached to the polymer (i.e. A' = A-M). The authors note that 1-M-A' is the fraction of all units in the polymer. The DB for hyperbranched polymers from the SCVP approach was higher for conversions less than 90% than the DB for hyperbranched polymers synthesized from condensation of AB₂ monomers (Figure 2.3). The lower DB at high conversion for hyperbranched polymers from SCVP was attributed to a nonequal distribution of A* and B*, which are the propagating radicals.

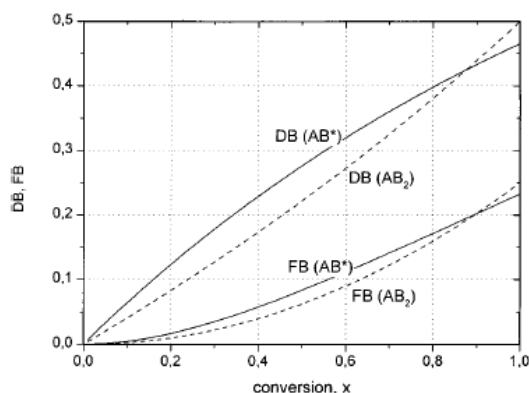


Figure 2.3: DB and fraction of branch points with conversion for SCVP hyperbranched polymers and AB₂ hyperbranched polymers⁵⁴

2.2.2 Degradation of Hyperbranched Polymers for Degree of Branching

Determination

The degree of branching, or the percent of monomeric units that contributed to branching is one of the most useful ways of describing hyperbranched polymers. Eqn (1) is traditionally used for the description of the DB.³⁶ Degree of branching is also useful in

examining steric or electronic effects on branching efficiency.^{63, 64} Branching and degree of branching was shown to have a significant effect on the physical properties.

The primary approach for determining the ratios of the dendritic, linear, and terminal groups is with ¹H or ¹³C NMR spectroscopy.^{65, 66} However, there are numerous instances where the resonances of the dendritic, linear, and terminal units are not well-resolved. Hölter et al. proposed an alternative calculation of degree of branching, which requires the resolution of only two of the three types of units⁶⁷:

$$DB = 2D/(2D + L) \approx 2T/(2T + L) \quad (5)$$

However, there still are hyperbranched polymers that do not have well-resolved resonances from either dendritic and linear units or terminal and linear units.

Kambouris et al. proposed an alternative to NMR spectroscopy for the determination of the ratio of dendritic, linear, and terminal units of hyperbranched polymers.⁶⁸ The new route to determining these ratios involved the degradation of the hyperbranched polymer bonds. The dendritic, linear, and terminal groups could be differentiated because the endgroups were modified prior to degradation. There are two conditions that are required for this process to accurately describe the ratio of the dendritic, linear, and terminal groups. First, the process for degrading the polymeric bonds must not adversely affect the modified endgroups. Second, the only products of the degradation must be the elementary subunits and complete degradation to these elementary subunits must occur. The subunits remaining after degradation of the polymer are then analyzed typically with a chromatographic technique such as HPLC or RP-HPLC.

The first use of the degradative process for degree of branching determination involved hyperbranched polyesters synthesized from the AB₂ monomer methyl 4,4-bis(4'-hydroxyphenyl)pentanoate. The hyperbranched polyester had hydroxyl endgroups, which were modified with methyl iodide and silver oxide to produce methoxy endgroups. The methoxy endgroups were hydrolytically stable while the ester linkages between subunits were not (Figure 2.4). After hydrolysis in a basic solution, the three subunits were detected with HPLC and the degree of branching was determined. The degree of branching (49%) was close to the theoretically predicted degree of branching for a statistical reaction (50%).⁶⁸

Another study that utilized the reductive degradation method for the determination of the degree of branching confirmed the results with ¹H NMR spectroscopy. Bolton et al. synthesized hyperbranched aryl polycarbonates with A₂B and AB₂ monomers, where the A₂B-based hyperbranched polymers had fluoroformate endgroups and the AB₂-based hyperbranched polymers had *tert*-butyldimethylsilyl ether endgroups.⁶⁹ Both aryl polycarbonates were treated with lithium aluminum hydride and the carbonate linkages were reduced to the subunits. The ratio of the subunits was determined with HPLC, and a degree of branching of approximately 50% was found for both hyperbranched polycarbonates. The ¹H NMR spectroscopy characterization of the degree of branching correlated well with the degree of branching determined through the reductive degradation process.⁶⁹

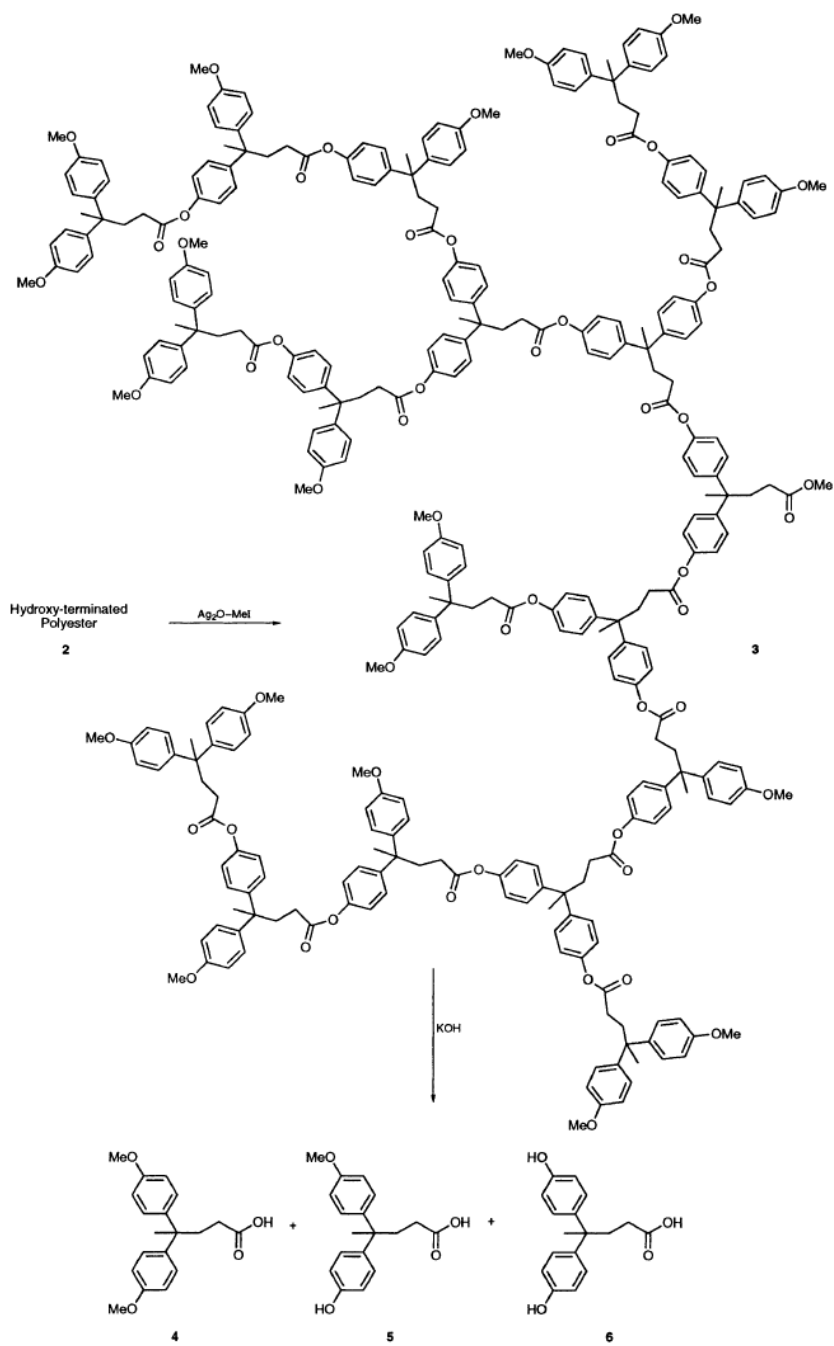


Figure 2.4: Endcapping and degradation of an aryl polyester for degree of branching analysis⁶⁹

The characterization of the degree of branching for hyperbranched lysine was performed with the reductive degradation technique. The hyperbranched lysine was

reduced to its subunits through hydrolysis. A combination of amino acid analysis and RP-HPLC was used to determine the ratios of dendritic, linear, and terminal subunits.⁷⁰

2.2.3 Indirect Methods for the Determination of the Degree of Branching

Another way to determine the degree of branching for hyperbranched polymers that do not have well-resolved NMR resonances or are degradable to distinct monomer units is the kinetic approach.⁷¹ Ishizu et al. used model compounds to determine the rate of initiation and propagation of the photopolymerization of 2-(N,N-diethyldithiocarbamyl)methylstyrene in benzene.⁷² The degree of branching was calculated from an equation proposed by Yan et al. for SCVP hyperbranched polymers.⁵⁴

Markoski et al. similarly tracked the development of the structure of hyperbranched polymers with model compounds. While the rate constants were not calculated in this study, a similar approach to Ishizu et al. was taken. An AB/AB₂ polymerization, where $0.25 > x_{AB} > 1.0$, was modeled with small molecules that could not polymerize but included A, B, and B₂ functionalities. The model compounds were reacted under similar conditions and stoichiometric ratios as for the polymerization. The products were analyzed with ¹H NMR spectroscopy and HPLC. The ratios of dendritic, linear, and terminal units were determined from the model compounds and reactions. The degree of branching was indirectly calculated from these ratios. For several compositions, the indirect method of degree of branching determination was verified with direct determination with ¹H NMR spectroscopy. These approaches provide useful alternatives to conventional analysis with NMR spectroscopy for the determination of the relative ratios of dendritic, linear, and terminal units in hyperbranched polymers.

2.2.4 Enhancement of the Degree of Branching

Hölter et al. found that the maximum DB for a hyperbranched polymer from an AB_2 monomer is 0.5, where the A and B groups have equal reactivity and a random reaction occurred.⁶⁷ The DB for a dendrimer is 1. To improve the DB of hyperbranched polymers, Hölter et al. proposed three approaches: a) higher reactivity of linear units compared to terminal units, b) polymerization of dendritic monomers, and c) slow addition of monomers.⁷³ Slow addition of monomers results in sequential addition of single monomer units, which leads to an improved degree of branching. The higher reactivity of linear units compared to terminal units greatly improved the degree of branching in the theoretical treatment of the system. For example, a DB of 0.8 was attainable when the linear unit was five times more reactive than the terminal.

Synthesis of hyperbranched polymers from prefabricated dendron monomers also enhanced the degree of branching. However, to achieve high DB, a high generation (> 8) of the dendron monomer was required. This tactic would theoretically result in high degrees of branching. However, there would be a high cost associated with the synthesis of dendritic monomers.

The final method for degree of branching enhancement was the slow addition of monomers. The ideal case, where AB_2 monomers are added slowly, was addressed. It was assumed that sterics did not influence the polymerization and that the coupling reaction was quantitative. The slow monomer addition led to an increase in the DB to 0.67.

Slow addition of monomers has a profound effect on the DB from A_2 plus B_3 polymerizations. Schmaljohann et al. evaluated the kinetics of hyperbranched A_2 plus B_3

polycondensations through calculation of differential equations using an iterative process.⁷⁴ It was determined that the most influential variable for the enhancement of DB was the slow addition of either both monomers or just the B₃ monomer to the A₂ (Figure 2.5). The reactivity of the B₃ units was important to the degree of branching, as well.

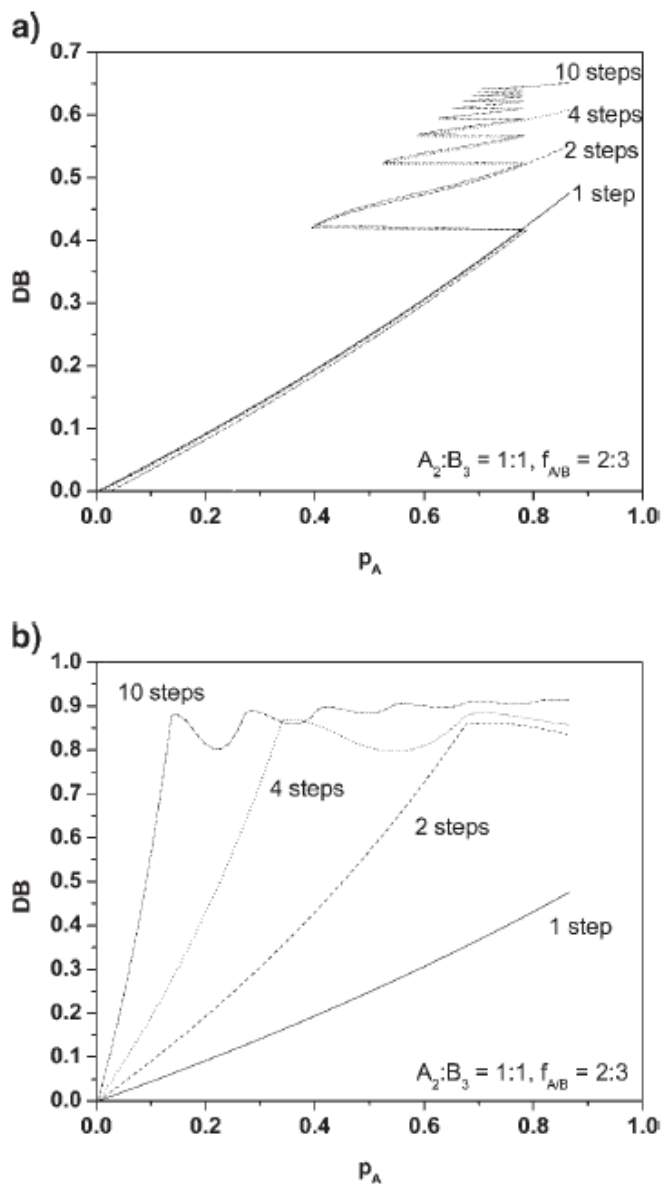


Figure 2.5: DB versus conversion for different steps of monomer addition a) simultaneous addition of A₂ and B₃, b) addition of B₃ to a solution of A₂⁷⁴

2.3 Molecular Weight Characterization of Hyperbranched Polymers

2.3.1 Characterization of Hyperbranched Polymers with Size Exclusion Chromatography

Size exclusion chromatography (SEC) is useful for the characterization of molecular weight and molecular weight distribution of linear polymers. This information is important for hyperbranched polymers, as well. A triple detector system with concentration, light scattering, and viscosity detectors provides the most detailed information about hyperbranched polymers.

The relationship between molecular weight and intrinsic viscosity is well-described with the Mark-Houwink equation for linear polymers.

$$[\eta] = k \cdot M_v^a \quad (1)$$

The constant, k , and exponent, a , have implications for the structure of the polymer. The Mark-Houwink exponent is typically in the range of 0.6 to 0.8 for flexible, linear polymers in a good solvent. Branched polymers frequently have Mark-Houwink exponents of less than 0.6 due to the more compact nature of branched polymers.⁷⁵ However, dendrimers do not follow this relationship. There is a maximum in the molecular weight versus intrinsic viscosity curve for dendritic polymers. Hyperbranched polymers are similar to dendritic polymers in that these polymers are globular and highly branched. However, hyperbranched polymers follow the Mark-Houwink relationship of molecular weight and intrinsic viscosity (Figure 2.6). The exponent, a , is smaller for hyperbranched polymers than linear analogs due to the more compact structure of

hyperbranched polymers.^{40, 41, 76, 77} Behera et al. synthesized a series of hyperbranched polyethers with different lengths of spacer segments between branch points. The hyperbranched polyether had a Mark-Houwink exponent of 0.37, which indicated a highly branched structure. As the spacer length increased from 0 to 10 carbons, the Mark-Houwink exponent increased from 0.37 to 0.54. With the introduction of longer distances between branch points, the polyethers were less branched, which was reflected in the much higher Mark-Houwink exponent for the polyethers.⁷⁸

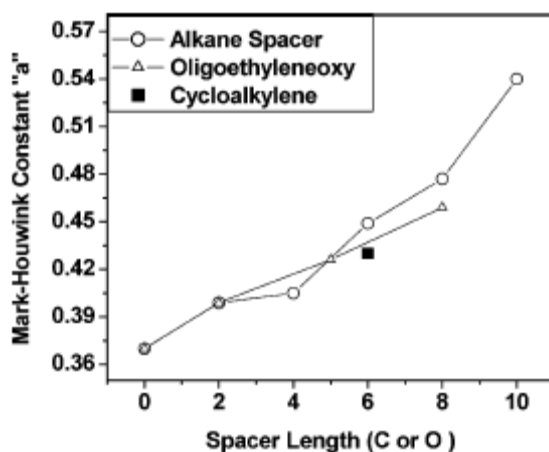


Figure 2.6: Variation of Mark-Houwink exponent with increasing spacer segment length in hyperbranched polyethers⁷⁸

Hyperbranched polymers from the step-growth polymerization of AB_x or A_2 and B_3 monomers have broad polydispersities (Figure 2.7).^{40, 79} Few studies have addressed the molecular weight distributions of hyperbranched polymers.

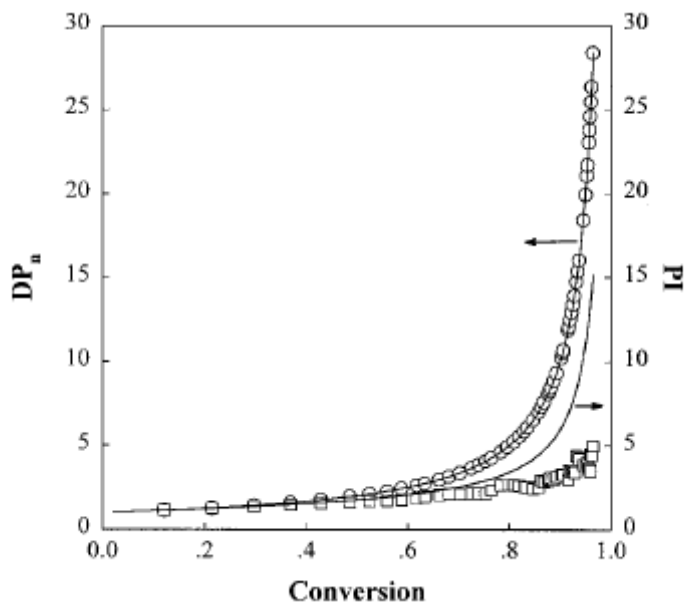
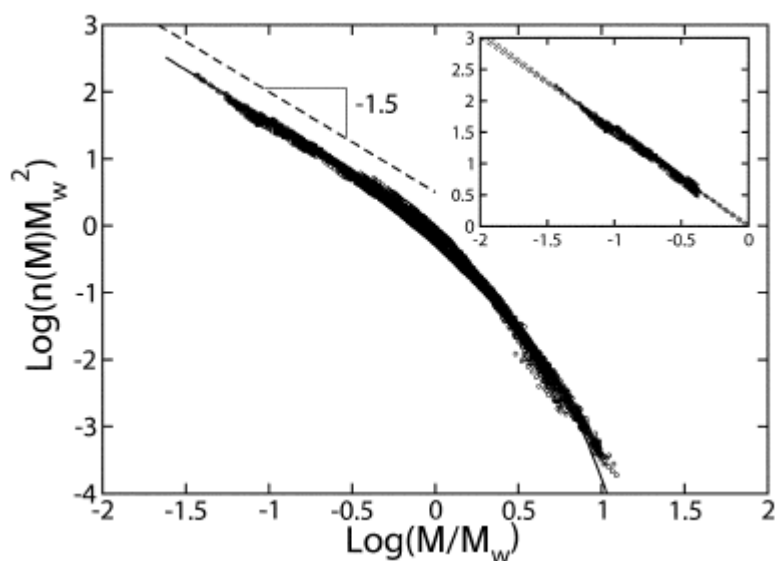


Figure 2.7: Number average degree of polymerization and polydispersity vs. conversion, where the solid lines are theoretical predictions⁷⁹

Kunamaneni et al. used an AB/AB₂ hyperbranched polymer system over a range of molecular weights (3,000 to 250,000 g/mol) to characterize the molecular weight distribution over a wide molecular weight range.⁸⁰ The hyperbranched polyesters showed a power law relationship between number density and molecular weight with an exponential cut-off at a characteristic upper cut-off mass, M_{char} , $n(M) \sim M^{-\tau} \times \exp(-M/M_{char})$. Rescaling of the data with M_w led to a universal curve for all of the hyperbranched polymers. This indicated that the hyperbranched polymers followed static scaling with τ and the ratio M_{char}/M_w , regardless of the molecular weight of the polymer. The value of τ was found to agree with mean-field scaling, which was surprising as percolation scaling was expected. Percolation scaling typically describes networks well. The disagreement with percolation scaling was attributed to a lower concentration of

loops for hyperbranched polymers when compared to networks.⁸⁰ The results agreed well with the recent scaling hypothesis proposed by Buzza for the molecular weight distribution of hyperbranched polymers, which follows a mean field theory.⁸¹ The fractal dimensions were also determined within this theoretical work.



Reproduced by permission of The Royal Society of Chemistry

Figure 2.8: Universal scaling plot, where τ is approximately 1.53⁸²

2.3.2 Characterization of Hyperbranched Polymers with Matrix Assisted Laser Desorption/Ionization-Time of Flight Mass Spectrometry (MALDI-TOF/MS)

Molecular weight characterization is traditionally performed with SEC. However, a useful technique for the molecular weight characterization of hyperbranched polymers is MALDI-TOF/MS. Several researchers have utilized MALDI-TOF/MS to confirm the molecular weights determined with SEC.⁸³ Muthukrishnan et al. synthesized

hyperbranched glycopolymers with a sugar-carrying acrylate. The molecular weights of the hyperbranched polymers ranged from 3,200 to 29,200 g/mol, which is within the range that MALDI-TOF/MS can reasonably be used for molecular weight determination. The polymers were first characterized with SEC/viscometry, and the molecular weights and dispersities were confirmed with MALDI-TOF/MS.⁸⁴

Cyclics form during the polymerization of hyperbranched polymers.¹⁵ The contribution of cyclics to the molecular weight distribution is difficult to determine with traditional techniques. While cyclics are a small contributor to the distribution of most hyperbranched polymers, even small amounts of cyclics can have a significant affect on physical properties of hyperbranched polymers. Kricheldorf et al. described in detail the contribution of cyclics to a wide variety of step-growth chemistries.⁸⁵ The authors made the distinction between thermodynamically and kinetically controlled polymerizations. Cyclization is more prevalent in kinetically controlled polymerizations. The authors advocate a modification of the classical theory from Flory⁴, which describes the polymerization of AB_x monomers, to account for cyclics in the distribution of hyperbranched polymers.

2.4 Rheological Behavior of Hyperbranched Polymers

Janzen and Colby¹⁷ aptly described the difficulty characterizing long-chain branching, which is defined as branches that are long enough to entangle. Determination of the presence and exact topologies of long-chain branched polymers, most notably polyethylene, is particularly difficult due to the sparse distribution of branch points.⁸⁶ Rheological characterization was one of the few characterization techniques to elucidate the structural differences among long-chain branched polymers.¹⁷ Hyperbranched

polymers have very high branching densities because each monomer presents an opportunity for branching. This topology differs significantly from long-chain branched polymers. The melt and solution rheological behavior of hyperbranched polymers received interest due to the unique architecture. Many techniques are useful for the elucidation of the molecular structures of hyperbranched polymers, and the flow behavior of hyperbranched polymers has proven useful as a complimentary technique for the determination of the molecular structure and intermolecular interactions.

2.4.1 Melt Rheology of Hyperbranched Polymers

Studies of the melt rheology of hyperbranched polymers have brought to light several trends for this topology. The first and most interesting point was that hyperbranched polymers are not entangled. The primary manifestation of the lack of entanglement with a power law of approximately 1.0 was the linear relationship between zero shear rate viscosity, η_0 , and weight-average molecular weight, M_w . The well-known η_0 - M_w relationship for linear polymers follows a power law relationship of approximately 1.0 for unentangled polymers and 3.4 for entangled polymers. Branching was shown to have a significant effect on this relationship.⁸⁷ Long-chain branching tends to create a greater dependence of η_0 on M_w when the molecular weight of the branch is sufficiently high to promote entanglements. Hyperbranched polymers are short-chain branched polymers and the preponderance of short chains impeded entanglements. This caused a weaker dependence of η_0 on M_w than expected for polymers of high molecular weight ($>10^6$ g/mol).⁹

Kharchenko et al.⁸⁸ synthesized linear, star, and hyperbranched polystyrenes for the investigation of the role of architecture on rheological behavior as well as the

conformation and orientation. The hyperbranched polystyrenes were synthesized through a controlled polymerization of styrene and divinylbenzene. The η_0 - M_w relationship was investigated for both linear and hyperbranched polymers of similar composition. The linear polystyrene followed the classical scaling of $M_w^{3.4}$ with η_0 . However, for comparable molecular weights, the hyperbranched polymers followed a weaker scaling of $M_w^{1.1}$ with η_0 (Figure 2.9). The weaker dependence was attributed to the high branching functionality and the disruption of entanglements by short branches. The hyperbranched polystyrene with a M_w of greater than 10^6 g/mol had distances between branch points greater than the critical molecular weight for entanglement, M_c , and agreed with the weak scaling of M_w with η_0 .⁸⁸

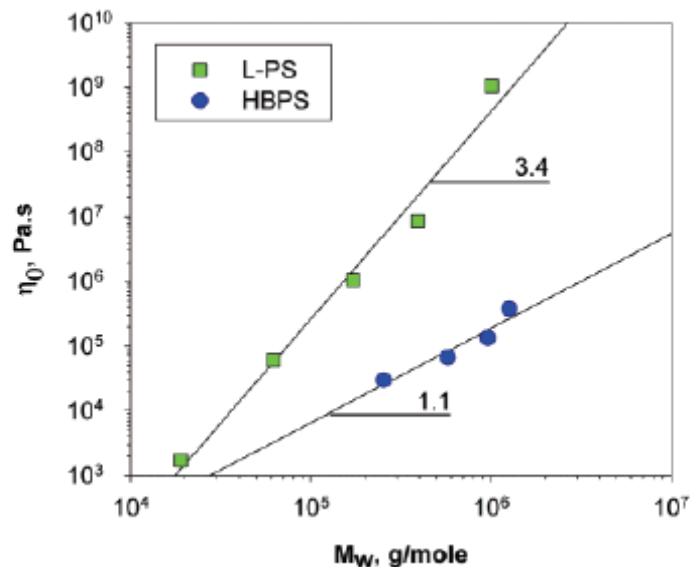


Figure 2.9: Weaker scaling of η_0 with M_w of hyperbranched polystyrene compared to linear polystyrene⁸⁸

Luciani et al. utilized commercially available aliphatic hyperbranched polyesters based on a tetrafunctional ethoxylated pentaerythritol core with 2,2-bis-

(hydroxymethyl)propionic acid repeating units to determine the effect of increasing molecular weight on η_0 .⁸⁹ Regardless of the experimental, the η_0 asymptotically approached scaling behavior of $M_w^{1.0}$ (Figure 2.10).

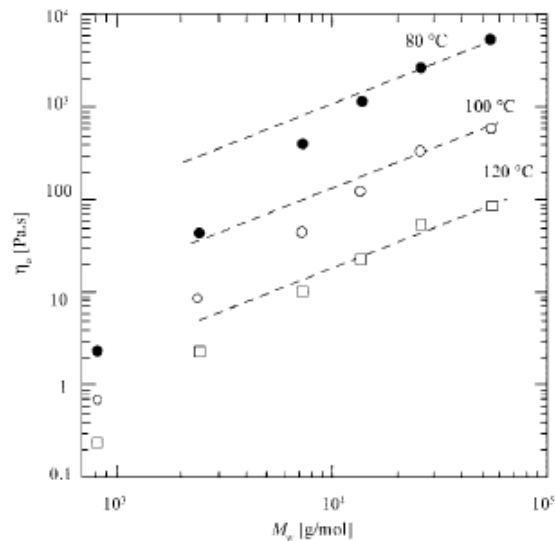


Figure 2.10: Relationship between η_0 and M_w for hyperbranched polyesters⁸⁹

The weak scaling of η_0 with M_w was attributed to Rouse-like behavior and a lack of entanglements in these polymers. The molecular weights of the hyperbranched polyesters were in the range of 2,400 to 55,510 g/mol.

While several studies attributed the weaker scaling of η_0 with M_w to Rouse-like behavior, modeling of the experimental data was not used to substantiate this observation.⁸⁹ Suneel et al. confirmed that hyperbranched polymers followed dynamic scaling based on Rouse-like behavior through an evaluation of experimental data with a

Rouse model.⁹ The hyperbranched polymers studied were synthesized with the AB₂ monomer 5-(hydroxyalkoxy)isophthalate. A hyperscaling relationship ($d_f = 3$) was consistent with the fractal dimension in the melt. The scaling was similar to that of near-critical gels.⁹⁰ While slow relaxation modes were observed in the terminal behavior of the hyperbranched polyesters, the slow relaxations were attributed to the ultrahigh molecular weight fraction of the distribution and not entanglements. The good fit of the dynamic scaling model based on the Rouse model to the experimental dynamic modulus data indicated that the hyperbranched polymers were unentangled polymeric fractals (Figure 2.11).⁹ The hyperbranched polyesters were fractionated and the rheological behavior was compared to the unfractionated hyperbranched polymer.⁸² The fractionated hyperbranched polyesters fit a dynamical scaling model based on the Rouse model, which incorporated the Schulz-Zimm parameterization of the molecular weight distribution. The authors concluded that the hyperbranched polymers regardless of molecular weight distribution were unentangled based on the good fit of the experimental data to the Rouse-based dynamic scaling model.⁸²

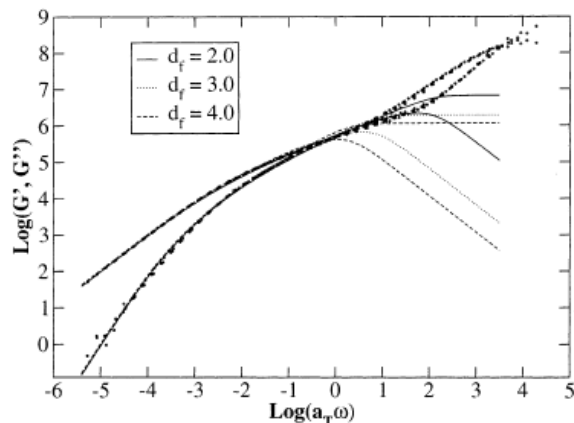


Figure 2.11: Good fit of Rouse-based dynamic scaling model to loss and storage modulus from hyperbranched polyesters indicating that the polyesters were unentangled⁹

Linear polymers frequently have η_0 's with Arrhenius temperature dependence, and the flow activation energy can be calculated from this relationship (1).

$$\eta_0(T) \propto \exp(E_a/RT) \quad (1)$$

Graessley observed that randomly long-chain branched polymers have higher flow activation energies than linear analogs.⁹¹ The higher activation energy corresponded to a slower cooperative diffusion of polymers in the melt.⁹² There are conflicting reports about the flow activation energy of hyperbranched polymers compared to linear analogs. The majority of studies dealing with the activation energy for flow in the melt indicated that hyperbranched polymers had higher activation energies than the comparable linear polymers.^{89, 93-95} However, Kwak et al.⁹⁶ and Choi et al.⁹⁷ found that for hyperbranched poly(ϵ -caprolactone), the activation energy decreased for branched polymers when compared to linear analogs (Figure 2.12). While those studies that indicated the activation energy increased for hyperbranched polymers were performed on different

chemistries (i.e. polyethylene and aliphatic polyester), the studies that showed that the activation energy for flow decreased from linear to branched polymers were both on the same poly(ϵ -caprolactone)s.^{89, 93-97} The authors attributed the higher flow activation energy to the high degree of branching in the hyperbranched polymers increasing the rigidity of the polymers.⁸⁹ The greater molecular mobility of hyperbranched poly(ϵ -caprolactone)s than linear poly(ϵ -caprolactone)s was speculated to be the cause of the lower flow activation energies for hyperbranched poly(ϵ -caprolactone)s.⁹⁶ Discrepancies in activation energy trends was also observed for branched polyesters.¹ This was attributed to differences in the temperature coefficients of linear and branched melts.⁹⁸

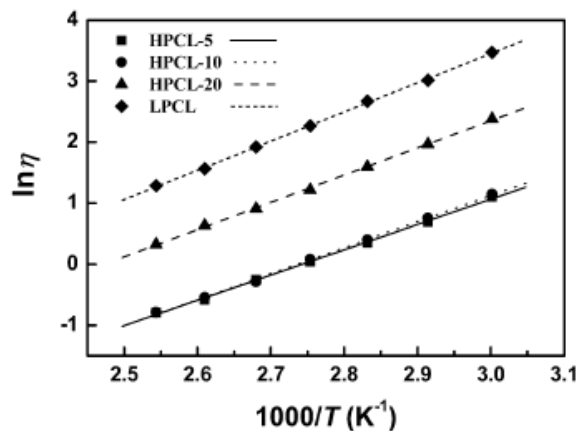


Figure 2.12: Temperature dependence of viscosity for hyperbranched poly(ϵ -caprolactone)s⁹⁷

Figure from (<http://www.sciencedirect.com/science/journal/00323861>)

Hyperbranched polymers have a periphery of functionality due to the high degree of branching, which creates a large number of endgroups (Figure 2.12).³³

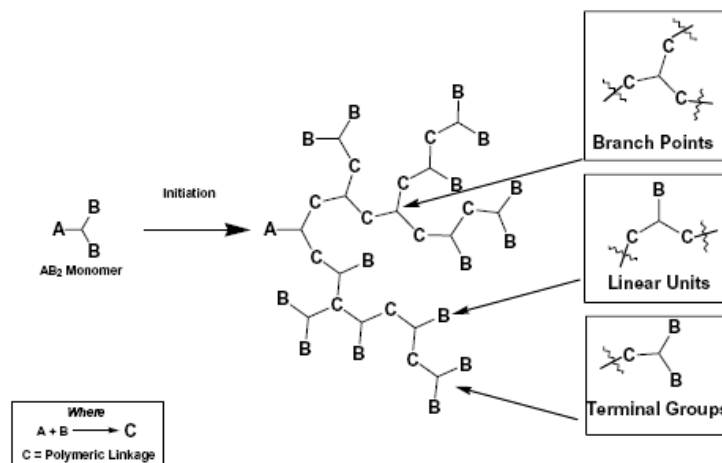


Figure 2.13: Illustration of hyperbranched polymer with a large number of terminal, B, groups³³

(Figure from <http://www.sciencedirect.com/science/journal/00143057>)

However, the influence of endgroups on the rheological properties of hyperbranched polymers has received sparse attention.⁹⁹ Dendritic poly(propylene imine)s were studied with methyl and benzyl acrylate endgroups.^{100, 101} After accounting for the changes in T_g with different endgroups, it was found that there was a maximum in the η_0 versus M_w curve for increasing bulk of the endgroup. One study on the influence of endgroups on the rheology of hyperbranched polymers focused on aliphatic hyperbranched polyesters with hydrogen-bonding endgroups. The endgroups of the aliphatic hyperbranched polyester were hydroxyl groups. The molecular weight and consequently the concentration of endgroups were changed. The lower molecular weight hyperbranched polyesters, which were those with the highest concentration of hydrogen bonding endgroups, had higher flow activation energy (Figure 2.14). The higher activation energy for flow in the melt was ascribed to the increased interaction of the hydrogen bonding

polyester endgroups when the concentration of these endgroups was greater as in the lower molecular weight polyesters.⁹³

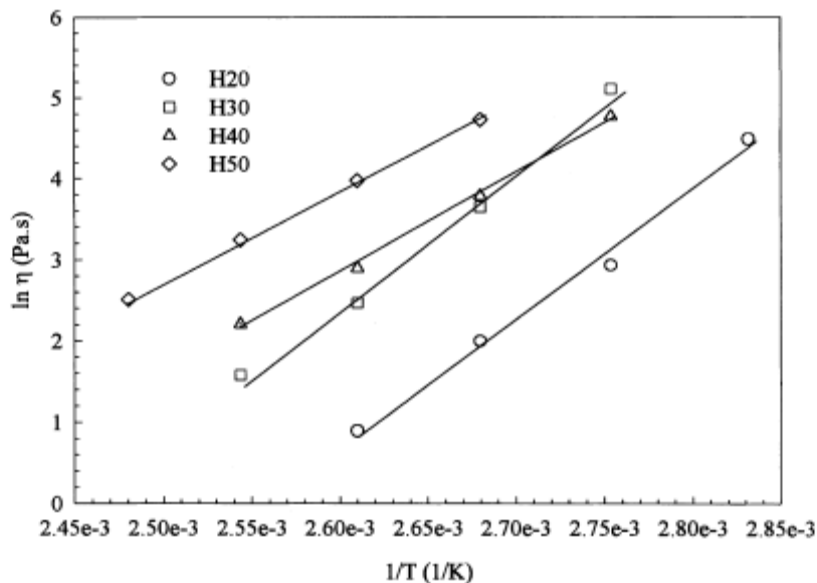


Figure 2.14: Influence of temperature on viscosity of hyperbranched polyesters with increasing molecular weight from sample H20 (2,100 g/mol) to H50 (7,500 g/mol)⁹³

Figure from (<http://www.sciencedirect.com/science/journal/00323861>)

The scaling of the loss, G'' , and storage, G' , moduli in the terminal zone has received significant attention in hyperbranched polymers. The terminal zone occurs at low frequency and is related to the relaxation mechanism of chain dynamics. For linear polymers, G'' scales directly with frequency, ω , and G' scales with ω^2 . Several studies have shown that hyperbranched polymers follow non-terminal scaling at low frequencies.⁹⁵ Kunamaneni et al. found for hyperbranched polyesters that the exponents for G'' scaling with frequency were in the range of 0.92 to 0.96 and 1.22 to 1.42 for G' .⁸² While exact dependencies varied for hyperbranched polymers, most researchers found

that G' and G'' for hyperbranched polymers were less dependent on frequency than linear counterparts (Figure 2.15).^{9, 96, 102, 103} Robertson et al. determined that hyperbranched polyisobutylene synthesized through the copolymerization of isobutylene and an inimer, 4-(2-methoxy-isopropyl) styrene (p-methoxycumyl styrene) reached terminal scaling only at very low frequencies.¹⁰⁴ However, the non-terminal scaling observed for most hyperbranched polymers has been observed for other non-linear topologies including dendritically branched polystyrenes¹⁰⁵, long-chain branched polyethylene¹⁰⁶, side chain dendritic poly(ether urethane)s¹⁰⁷, and multiarm polybutadiene and polyisoprene stars¹⁰⁸. The non-terminal scaling for the moduli was typically attributed to long relaxation times occurring in these topologies during the low frequencies. The source of these long relaxations seems to remain undetermined. It is generally agreed, however, that the source of these relaxations was not due to a physical structure. Generally, the behavior was attributed to a modification of relaxation behavior.

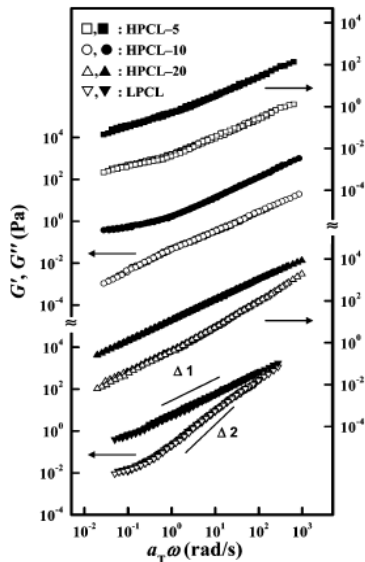


Figure 2.15: Non-terminal scaling of hyperbranched poly(ϵ -caprolactone)s⁹⁶

Many researchers also noted that no intersection of G' and G'' was observed in the terminal region for hyperbranched polymers. The longest relaxation time is calculated from this intersection.¹⁰⁹ The absence of an intersection was interpreted as an indication of a lack of entanglements in hyperbranched polymers.^{9,96}

The lack of entanglements in hyperbranched polymers results in lower melt viscosity compared to linear analogs.^{88,110} The significant reduction in melt viscosity of hyperbranched polymers compared to linear analogs has made hyperbranched polymers interesting for several applications. Blends with linear polymers, not necessarily of similar chemistry, as an aid for polymer processing has been explored.^{13,111,112}

The rheological behavior of hyperbranched polymers has given insight into the intermolecular interactions. Most evidence from melt rheology of hyperbranched polymers pointed to a lack of entanglements for this topology. The relationship between η_0 and M_w was much weaker than for linear, entangled analogs, which indicated that the hyperbranched polymers remained unentangled even at molecular weights above 1,000,000 g/mol. The flow behavior of hyperbranched polymers exhibited Rouse-like behavior. No crossover between G' and G'' in the terminal region was observed, which indicated that no entanglements were present in the hyperbranched polymers. Non-terminal behavior was observed for G' and G'' at low frequencies. However, the cause of the non-terminal behavior has yet to be determined.

2.4.2 Solution Rheological Behavior of Hyperbranched Polymers

Several studies focused on the solution rheological behavior of hyperbranched polymers. Nunez et al. used hyperbranched aliphatic polyesters dissolved in 1-methyl-2-pyrrolidinone for the determination of solution rheological behavior.¹¹³ The

hyperbranched polyesters exhibited Newtonian behavior over the shear rates examined and at all concentrations, which ranged from 10 to 50 wt%. The solution viscosity increased slightly with higher generation of the hyperbranched polyester. Star-shaped polymers have exhibited relative independence of solution rheological behavior with molecular weight, also.¹¹⁴ The authors also blended the hyperbranched polyesters with linear poly(2-hydroxyethyl methacrylate), and significant decreases in the solution viscosity of the blends was observed compared to the linear polymer solution. However, it is important to note that the molecular weight of the linear polymer was much higher, approximately 300,000 g/mol, than the hyperbranched additives, which ranged in molecular weight from 1,750 to 14,600 g/mol. Therefore, the authors of this review believe it is difficult to discern the impact of the globular structure of the hyperbranched polymer on the solution behavior of the blends.

Thompson et al. observed that a decrease in the degree of branching of hyperbranched poly(ether imide)s resulted in an earlier onset of shear thinning for 40 wt% solutions. The onset of normal stresses also increased with a decrease in the degree of branching. The rheo-optics indicated that the hyperbranched poly(ether imide) with the lowest degree of branching had the greatest birefringence, and the hyperbranched poly(ether imide) with the highest degree of branching exhibited the lowest birefringence. Birefringence is a result of the optical anisotropy of sheared polymers and is proportional to the degree of entanglement. The trend of decreasing birefringence with increasing branching is consistent with the hyperbranched polymers with a higher degree of branching having a globular, unentangled structure.¹¹⁵

2.5 Thermal Properties of Hyperbranched Polymers

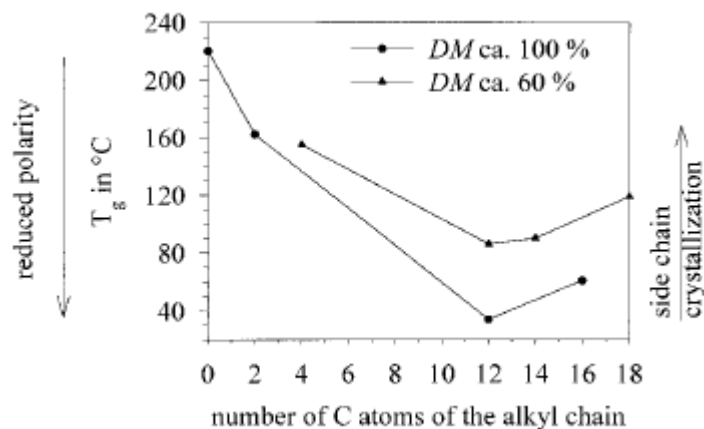
A number of factors contribute to the different thermal properties of hyperbranched polymers compared to linear or even long-chain branched polymers. The increase in the number of endgroups can affect the degradation rate, if the endgroups play a role in degradation of the polymer, and the increased movement and free volume from a higher concentration of endgroups compared to linear or long-chain branched analogs can affect the thermal properties of the hyperbranched polymers.

2.5.1 Influence of Endgroups on Glass Transition of Hyperbranched Polymers

While endgroups influence the thermal properties of linear polymers, especially low molecular weight linear polymers, the effect of endgroups on thermal properties for hyperbranched polymers is more pronounced due to the periphery of endgroups. For a hyperbranched polymer of the same chemical structure, degree of branching, and similar molecular weight, bulky endgroups hinder chain motion and increase the T_g . Elrehim et al. synthesized hyperbranched poly(urethane urea)s through an AA^* plus B^*B_2 and endcapped the hydroxyl endgroup with either an aromatic or aliphatic isocyanate.¹¹⁶ The T_g increased by approximately 30 °C when the bulky phenyl group was replaced with an aliphatic group. The ability to adjust the T_g significantly through slight modifications of the endgroup provides versatility for applications of hyperbranched polymers.

While the structure of endgroups was found to have an affect on the thermal transitions of hyperbranched polymers, differences in polarity and hydrogen bonding capability of endgroups has even greater influence on thermal transitions.^{11, 117, 118} The

large changes in thermal transitions observed for changes in the polarity or hydrogen bonding capability of hyperbranched polymers has led to significant interest. The size of flexible endgroups, which reduce the effectiveness of hydrogen bonding, also influences the T_g of hyperbranched polymers. Schmaljohann et al. found that increasing the length of the alkyl endcapper of aromatic hyperbranched polyesters originally endcapped with hydroxyl groups dramatically decreased the T_g of the hyperbranched polymers (Figure 2.16). The decrease in T_g with increasing alkyl length was attributed to a reduction in hydrogen bonding capability. The crystallization of the long alkyl ($>C_{12}$) endgroups led to intramolecular phase separation. The T_g was found to increase once the length of the alkyl endcapper had exceeded C_{12} , which was associated with the crystallization of the long alkyl chains. An increase in the number of hydroxyl endgroups endcapped with long alkyl chains also caused a significant decrease in the T_g of the hyperbranched polyester. The reduction in intermolecular interactions caused greater mobility at lower temperatures and a lower T_g (Figure 2.16).



Reproduced by permission of The Royal Society of Chemistry

Figure 2.16: Influence of the increasing length of alkyl endcapper, which reduced the hydrogen bonding capability, on T_g of an aromatic hyperbranched polyester⁶⁸

Baek et al. made a direct comparison of hyperbranched poly(phenylquinoxaline)s with different endgroups having different polarity.¹¹⁹ The poly(phenylquinoxaline)s were terminated with either hydroxyl groups, which had hydrogen bonding capability, or with fluorine, a non-polar functionality. The effect of these endgroups on the thermal properties was investigated. Linear analogs of the hydroxyl- and fluorine-terminated poly(phenylquinoxaline)s were synthesized for comparison, as well. Little difference was observed between the T_g 's of fluorine-terminated linear and hyperbranched poly(phenylquinoxaline)s (220 and 225 °C, respectively). However, the T_g of the hydroxyl-terminated hyperbranched poly(phenylquinoxaline)s was approximately 50 °C higher than the linear analog. Among the hyperbranched poly(phenylquinoxaline)s the hydroxyl-terminated polymer had a T_g that was approximately 75 °C higher than the fluorine-terminated hyperbranched

poly(phenylquinoxaline). The large number of endgroups provided a useful route to the modification of the thermal behavior of the polymers without changing the backbone chemistry. The glass transition temperature could also be used as a tool to detect differences in endgroups of hyperbranched polymers.

The incorporation of linear units into the hyperbranched polymer was carried out through changing the ratio of AB:AB₂ monomers from 0:100 to 100:0. As the topology of the polymer shifted from hyperbranched to linear, the T_g of the hydroxyl-terminated polymers gradually decreased with the reduction in hydrogen bonding endgroups. The gradual change in topology from hyperbranched to linear resulted in little difference in terms of T_g for the fluorine-terminated polymers. The degradation temperature for 5 % weight loss for the fluorine-terminated polymers over the range of topologies were all quite similar. The hydroxyl-terminated poly(phenylquinoxaline)s was dependent on the number of endgroups, where those with more hydroxyl endgroups were less thermally stable.¹¹⁹

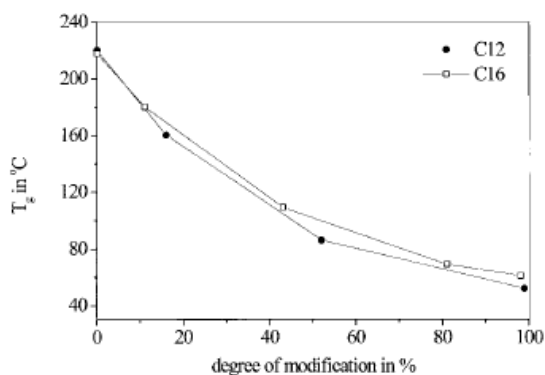
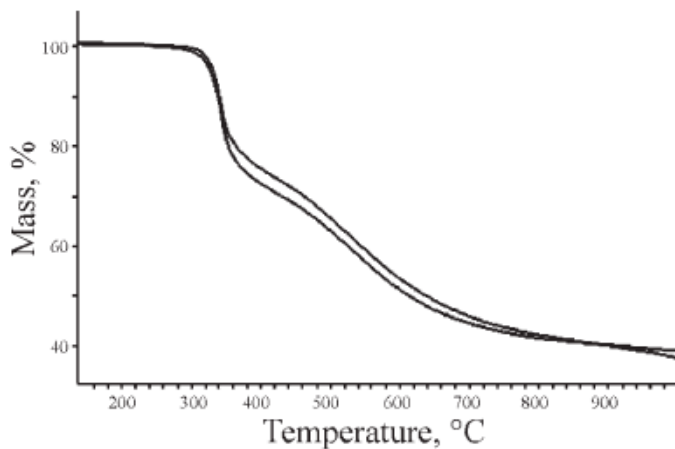


Figure 2.17: Reduction in T_g with replacement of hydroxyl, hydrogen bonding, endgroups with alkyl, non-polar, endgroups¹¹⁸

2.5.2 Thermal Stability of Hyperbranched Polymers

Hyperbranched polymers, where the chemical structure of the polymer is typically thermally stable, remained thermally stable despite the increase in the number of endgroups and branching (e.g. polyarylenes) (Figure 2.18).¹²⁰⁻¹²² However, changes in endgroup chemistry affects the thermal stability of hyperbranched polymers. Terminal groups with hydrogen bonding capability produced different trends in thermal stability based on the backbone chemistry of the polymers. While hyperbranched poly(amino esters) increased the temperature at which 5 % weight loss occurred with a decrease in hydrogen bonding capability, the opposite trend was observed for poly(phenylquinoxaline)s.^{119, 123} Fossum and Tan synthesized linear poly(arylene ether ketone)-*co*-hyperbranched poly(arylene ether oxide) copolymers. The thermal stability of the copolymers was improved significantly with the incorporation of the hyperbranched poly(arylene ether oxide). This effect was attributed to the greater thermal stability of triarylphosphine oxide than the linear homopolymer.¹²⁴ The thermal stability of hyperbranched polymers depends significantly on the chemical structure of the polymer and endgroups. However, the impact of the endgroup's thermal stability is magnified for hyperbranched polymers when compared to linear counterparts.



Reproduced by permission of The Royal Society of Chemistry

Figure 2.18: Good thermal stability of two hyperbranched fluoropolymers¹²¹

2.5.3 Impact of Hyperbranched Topology on Crystallization

Structural symmetry is a requirement for crystallization in polymers. Disruption of symmetry, whether from a kink in the structure due to the chemistry or a branch point, will disrupt crystallinity in a polymeric system.¹²⁵ While branching in polymers at low levels is known to reduce the degree of crystallinity, the much greater degree of branching in hyperbranched polymers contributed to a greater influence on the crystallinity than traditional long-chain branched polymers.¹²⁶ Hyperbranched polymers are frequently weakly crystalline or amorphous when the linear analogs are semi-crystalline with a high degree of crystallinity.^{30, 127, 128}

Mai et al. demonstrated that a systematic change in the degree of branching while the molecular weight remained constant of hyperbranched polymers greatly affects polymer crystallization.¹²⁹ A series of hyperbranched poly[3-ethyl-3-(hydroxymethyl)oxetane] (PEHO) with degrees of branching ranging from 5.6 to 45%

were characterized with ^{13}C NMR spectroscopy, SEC, XRD, and DSC. Others have shown that with higher degrees of branching, a reduction in crystallinity is observed for hyperbranched polymers.^{130, 131} However, these studies did not control the molecular weight while changing the degree of branching. Therefore, molecular weight effects could not be disregarded for the previous studies. A decrease in the relative degree of crystallinity with increasing degree of branching was observed (Figure 2.19). Also, an increase in linear units led to an increase in the degree of crystallinity while an increase in dendritic and terminal units had the opposite effect.¹²⁹

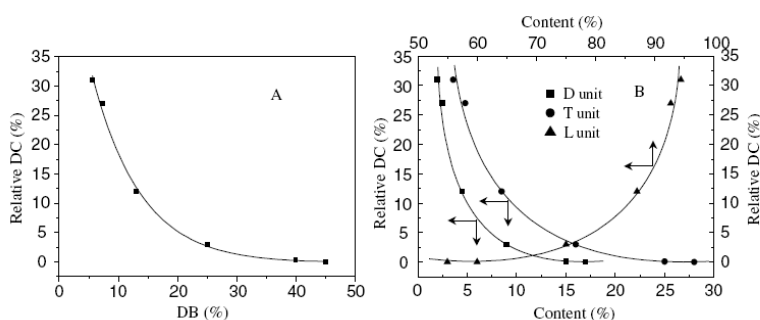


Figure 2.19: Influence of the degree of branching on the relative degree of crystallinity and the influence of dendritic, linear, and terminal units on the relative degree of crystallinity¹²⁹

Large degrees of branching were shown to disrupt crystallinity. However, the endgroup of hyperbranched polymers can have an effect on crystallization in the system, as well. It was shown that crystallinity was disrupted by branching in the bulk of the hyperbranched polymers. However, endcapping the hyperbranched polymer with long alkyl groups (> 12 carbons) can lead to crystallization of the endgroups.^{116, 132}

2.6 References

1. McKee, M. G.; Wilkes, G. L.; Colby, R. H.; Long, T. E. *Macromolecules* **2004** 37, 1760-1767.
2. McLeish, T. C. B.; Milner, S. *Adv. Polym. Sci.* **1999** 143, 195-256.
3. Flory, P. J. *J. Am. Chem. Soc.* **1941** 63, 3083-3090.
4. Flory, P. J. *J. Am. Chem. Soc.* **1952** 74, 2718-2723.
5. Scherrenberg, R.; Coussens, B.; van Vilet, P.; Edouard, G.; Brackman, J.; de Brabander, E. *Macromolecules* **1998** 31, 456-461.
6. Mourey, T. H.; Turner, S. R.; Rubenstein, M.; Freché, J. M. J.; Hawker, C. J.; Wooley, K. L. *Macromolecules* **1992** 25, 2401-2406.
7. Uppuluri, S.; Keinath, S. E.; Tomalia, D. A.; Dvornic, P. R. *Macromolecules* **1998** 31.
8. Suneel; Buzza, D. M. A.; Groves, D. J.; McLeish, T. C. B.; Parker, D.; Keeney, A. J.; Feast, W. J. *Macromolecules* **2002** 35, 9605-9612.
9. Hawker, C. J.; Farrington, P. J.; Mackay, M. E.; Wooley, K. L.; Fréchet, J. M. J. *J. Am. Chem. Soc.* **1995** 117, 4409-4410.
10. Kim, Y. H.; Webster, O. W. *Macromolecules* **1992** 25, 5561-5572.
11. Hsieh, T.-T.; Tiu, C.; Simon, G. P. *Polymer* **2001** 42, 7635-7638.
12. Hong, Y.; Cooper-White, J. J.; Mackay, M. E.; Hawker, C. J.; Malmstrom, E.; Rehnberg, N. *J. Rheol.* **1999** 43, 781-793.
13. Mulkern, T. J.; Beck Tan, N. C. *Polymer* **2000** 41, 3193-3203.
14. Unal, S.; Lin, Q.; Mourey, T. H.; Long, T. E. *Macromolecules* **2005** 38, 3246-3254.
15. McKee, M. G.; Park, T.; Unal, S.; Yilgor, I.; Long, T. E. *Polymer* **2005** 46, 2011-2015.
16. Unal, S.; Oguz, C.; Yilgor, E.; Gallivan, M.; Long, T. E.; Yilgor, I. *Polymer* **2005** 46, 695-696.

17. Unal, S.; Yilgor, I.; Yilgor, E.; Sheth, J. P.; Wilkes, G. L.; Long, T. E. *Macromolecules* **2004** *37*, 7081-7084.
18. Janzen, J.; Colby, R. H. *J. Mol. Struct.* **1999** 485-486, 569-584.
19. Zimm, B. H.; Stockmayer, W. H. *J. Chem. Phys.* **1949** *17*, 1301-1314.
20. Radke, W.; Müller, A. H. E. *Macromolecules* **2005** *38*, 3949-3960.
21. Flory, P. J., In *Principles of Polymer Chemistry*. 16th ed.; Cornell University Press: Ithaca, NY, 1986.
22. Zimm, B. H.; Kilb, R. W. *J. Polym. Sci.* **1959** *37*, 19-42.
23. Berry, G. C. *J. Polym. Sci., Polym. Phys. Ed.* **1968** *6*, 1551-1554.
24. Berry, G. C. *J. Polym. Sci.: Part B: Polym. Phys.* **1988** *35*, 1377-1397.
25. Radke, W.; Gerber, J.; Wittmann, G. *Polymer* **2003** *44*, 519-525.
26. Tackx, P.; Tackx, J. C. J. F. *Polymer* **1998** *39*, 3109-3113.
27. Kraus, G.; Stacy, C. J. *J. Polym. Sci., Polym. Phys. Ed.* **1972** *10*, 657-672.
28. Gupta, P.; Wilkes, G. L.; Sukhadia, A. M.; Krishnaswamy, R. K.; Lamborn, M. J.; Wharry, S. M.; Tso, C. C.; DesLauriers, P. J.; Mansfield, T.; Beyer, F. L. *Polymer* **2005** *46*, 8819-8837.
29. Voit, B. *J. Polym. Sci.: Part A: Polym. Chem.* **2005** *43*, 2679-2699.
30. Voit, B. *J. Polym. Sci.: Part A: Polym. Chem.* **2000** *38*, 2505-2525.
31. Jikei, M.; Kakimoto, M. *Prog. Polym. Sci.* **2001** *26*, 1233-1285.
32. Gao, C.; Yan, D. *Prog. Polym. Sci.* **2004** *29*, 183-275.
33. Kim, Y. H. *J. Polym. Sci.: Part A: Polym. Chem.* **1998** *36*, 1685-1698.
34. Yates, C. R.; Hayes, W. *Eur. Polym. J.* **2004** *40*, 1257-1281.
35. Flory, P. J. *J. Am. Chem. Soc.* **1952** *74*, 2718-2723.
36. Urich, K. E.; Hawker, C.; Fréchet, J. M. J.; Turner, S. R. *Macromolecules* **1992** *25*, 4583-4587.
37. Hawker, C. J.; Lee, R.; Fréchet, J. M. J. *J. Am. Chem. Soc.* **1991** *113*, 4583-4588.

38. Malmstrom, E.; Johansson, M.; Hult, A. *Macromolecules* **1995** 28, 1698-1703.
39. Yang, G.; Jikei, M.; Kakimoto, M. *Macromolecules* **1999** 32, 2215-2220.
40. Kumar, A.; Ramakrishnan, S. *J. Chem. Soc., Chem. Commun.* **1993**, 1453-1454.
41. Turner, S. R.; Voit, B. I.; Mourey, T. H. *Macromolecules* **1993** 26, 4617-4623.
42. Turner, S. R.; Walter, F.; Voit, B. I.; Mourey, T. H. *Macromolecules* **1994** 27, 1611-1616.
43. Massa, D. J.; Shriner, K. A.; Turner, S. R.; Voit, B. I. *Macromolecules* **1995** 28, 3214-20.
44. Morgenroth, F.; Müllen, K. *Tetrahedron* **1997** 45, 15349-15366.
45. Fukuzaki, E.; Nishide, H. *J. Am. Chem. Soc.* **2005** 128, 996-1001.
46. Hobson, L. J.; Kenwright, A. M.; Feast, W. J. *Chem. Comm.* **1997** 1877-1879.
47. Chikh, L.; Arnaud, X.; Guillermain, C.; Tessier, M.; Fradet, A. *Macromol. Symp.* **2003** 199, 209-221.
48. Zagar, E.; Zigon, M.; Podzimek, S. *Polymer* **2006** 47, 166-175.
49. Burgath, A.; Sunder, A.; Frey, H. *Macromol. Chem. Phys.* **2000** 201, 782-791.
50. Müller, A. H. E.; Yan, D.; Wulkow, M. *Macromolecules* **1997** 30, 7015-7023.
51. Cheng, K.-C. *Polymer* **2003** 44, 877-882.
52. Simon, P. F. W.; Müller, A. H. E. *Macromol. Theory Simul.* **2000** 9, 621-627.
53. Mori, H.; Walther, A.; Andre, X.; Lanzendoerfer, M. G.; Müller, A. H. E. *Macromolecules* **2004** 37, 2054-2066.
54. Ivan, B.; Erd-di, G.; Kali, G.; Hollo-Szabo, G.; Zsebi, Z.; Szesztay, M. In *New functional hyperbranche and star polymers*, 228th ACS National Meeting, Philadelphia, PA, August 22-26, 2004; PMSE: Philadelphia, PA, 2004.
55. Jin, M.; Lu, R.; Bao, C.; Xu, T.; Zhao, Y. *Polymer* **2004** 45, 1125-1131.
56. In, I.; Kim, S. Y. *Macromol. Chem. Phys.* **2005** 206, 1862-1869.

57. Chang, Y.-T.; Shu, C.-F.; Leu, C.-M.; Wei, K.-H. *J. Polym. Sci.: Part A: Polym. Chem.* **2003** 41, 3726-3735.
58. Wu, F.-I.; Shu, C.-F. *J. Polym. Sci.: Part A: Polym. Chem.* **2001** 39, 3851-3860.
59. Flory, P. J., In *Principles of Polymer Chemistry*. Cornell University Press: Ithaca, NY, 1953.
60. Kim, Y. H.; Webster, O. W. *J. Am. Chem. Soc.* **1990** 112, 4592-4593.
61. Hao, J.; Jikei, M.; Kakimoto, M. *Macromolecules* **2003** 36, 3519-3528.
62. Cheng, K.-C. *Polymer* **2003** 44, 1259-1266.
63. Li, X.; Yuesheng, L.; Tong, Y.; Shi, L.; Liu, X. *Macromolecules* **2003** 36, 5537-5544.
64. Yan, D.; Müller, A. H. E.; Matyjaszewski, K. *Macromolecules* **1997** 30, 7024-7033.
65. Hanselmann, R.; Hoelter, D.; Frey, H. *Macromolecules* **1998** 31, 3790-3801.
66. Hawker, C. J.; Chu, F. *Macromolecules* **1996** 29, 4370-4380.
67. Zhang, J.; Wang, H.; Li, X. *Polymer* **2006** 47, 1511-1518.
68. Blencowe, A.; Davidson, L.; Hayes, W. *Eur. Polym. J.* **2003** 39, 1955-1963.
69. Hölder, D.; Burgath, A.; Frey, H. *Acta Polymer.* **1997** 48, 30-35.
70. Kambouris, P.; Hawker, C. J. *J. Chem. Soc. Perkin Trans. I* **1993**, 2717-2721.
71. Bolton, D. H.; Wooley, K. L. *J. Polym. Sci.: Part A: Polym. Chem.* **2002** 40, 823-835.
72. Menz, T. L.; Chapman, T. *Polym. Prep.* **2003** 44, 842-843.
73. Ishizu, K.; Ohta, Y.; Kawauchi, S. *Macromolecules* **2002** 35, 3781-3784.
74. Ishizu, K.; Ohta, Y.; Kawauchi, S. *J. Appl. Polym. Sci.* **2005** 96, 1810-1815.
75. Höelter, D.; Frey, H. *Acta Polymer.* **1997** 48, 298-309.
76. Schmaljohann, D.; Voit, B. *Macromol. Theory Simul.* **2003** 12, 679-689.

77. Garamszegi, L.; Nguyen, T.; Plummer, C. J. G.; Månson, J.-A. E. *J. Liq. Chrom. Related Tech.* **2003** 26, 207-230.
78. Li, J.; Gauthier, M. *Macromolecules* **2001** 34, 8918-8924.
79. Pavlov, G. M.; Errington, N.; Harding, S. E.; Korneeva, E. V.; Roy, R. *Polymer* **2001** 42, 3671-3678.
80. De Luca, E.; Richards, R. W. *J. Polym. Sci.: Part B: Polym. Phys.* **2003** 41, 1339-1351.
81. Yamaguchi, N.; Wang, J.-S.; Hewitt, J. M.; Lenhart, W. C.; Mourey, T. H. *J. Polym. Sci.: Part A: Polym. Chem.* **2002** 40, 2855-2867.
82. Behera, G. C.; Ramakrishnan, S. *Macromolecules* **2004** 37, 9814-9820.
83. Lee, Y. U.; Jang, S. S.; Jo, W. H. *Macromol. Theory Simul.* **2000** 9, 188-195.
84. Kunamaneni, S.; Buzza, D. M. A.; Parker, D.; Feast, W. J. *J. Mater. Chem.* **2003** 13, 2749-2755.
85. Buzza, D. M. A. *Eur. Phys. J. E* **2004** 13, 79-86.
86. Jayakannan, M.; Van Dongen, J. L. J.; Behera, G. C.; Ramakrishnan, S. *J. Polym. Sci.: Part A: Polym. Chem.* **2002** 40, 4463-4476.
87. Muthukrishnan, S.; Jutz, G.; André, X.; Mori, H.; Müller, A. H. E. *Macromolecules* **2005** 38, 9-18.
88. Sun, X.; Moreira, R. G. *J. Food Proc. Pres.* **1996** 20, 157-167.
89. Muenstedt, H.; Dietmar, A. *J. Non-Newtonian Fluid Mech.* **2005** 128, 62-69.
90. Kharchenko, S. B.; Kannan, R. M.; Cernohous, J. J.; Venkataramani, S. *Macromolecules* **2003** 36, 399-406.
91. Luciani, A.; Plummer, C. J. G.; Nguyen, T.; Garamszegi, L.; Månson, J.-A. E. *J. Polym. Sci.: Part B: Polym. Phys.* **2004** 42, 1218-1225.
92. Colby, R. H.; Gillmor, J. R.; Rubenstein, M. *Phys. Rev. E: Stat. Phys., Plasmas, Fluids, Relat. Interdiscip. Top.* **1993** 48, 3712-3716.
93. Kunamaneni, S.; Buzza, D. M. A.; De Luca, E.; Richards, R. W. *Macromolecules* **2004** 37, 9295-9297.
94. Graessley, W. W. *Macromolecules* **1982** 15, 1164-1167.

95. Bailey, R. T.; North, A. M.; Pethrick, R. A., In *Molecular Motion in High Polymers*. Oxford University Press: New York, 1981.
96. Hsieh, T.-T.; Tiu, C.; Simon, G. P. *Polymer* **2001** 42, 1931-1939.
97. Ye, Z.; Zhu, S. *Macromolecules* **2003** 36, 2194-2197.
98. Ye, Z.; AlObaidi, F.; Zhu, S. *Macromol. Chem. Phys.* **2004** 205, 897-906.
99. Kwak, S.-Y.; Choi, J.; Song, H. J. *Chem. Mater.* **2005** 17, 1148-1156.
100. Choi, J.; Kwak, S.-Y. *Polymer* **2004** 45, 7173-7183.
101. Böhme, F.; Clausnitzer, C.; Gruber, F.; Grutke, S.; Huber, T.; Pötschke, P.; Voit, B. *High Perform. Polym.* **2001** 13, 21-31.
102. Tande, B. M.; Wagner, N. J.; Kim, Y. H. *Macromolecules* **2003** 36, 4619-4623.
103. Sendijarevic, I.; McHugh, A. J. *Macromolecules* **2000** 33, 590-596.
104. Kharchenko, S. B.; Kannan, R. M.; Cernohous, J. J.; Venkataramani, S.; Babu, G. N. *J. Polym. Sci.: Part B: Polym. Phys.* **2001** 39, 2562-2571.
105. Simon, P. F. W.; Müller, A. H. E.; Pakula, T. *Macromolecules* **2001** 34, 1677-1684.
106. Robertson, C. G.; Roland, C. M.; Puskas, J. E. *J. Rheol.* **2002** 46, 307-320.
107. Dorgan, J. R.; Knauss, D. M.; Al-Muallem, H. A.; Huang, T.; Vlassopoulos *Macromolecules* **2003** 36, 380-388.
108. García-Franco, C. A.; Srinivas, S.; Lohse, D. J.; Brant, P. *Macromolecules* **2001** 34, 3115-3117.
109. Jahromi, S.; Palman, J. H. M.; Steeman, P. A. M. *Macromolecules* **2000** 33, 577-581.
110. Pakula, T.; Vlassopoulos, D.; Fytas, G.; Roovers, J. *Macromolecules* **1998** 31, 8931-8940.
111. Rubenstein, M.; Colby, R. H., In *Polymer Physics*. Oxford University Press: New York, 2003.
112. Gretton-Watson, S. P.; Alpay, E.; Steinke, J. H. G.; Higgins, J. S. *Ind. Eng. Chem. Res.* **2005** 44, 8682-8693.

113. Plummer, C. J. G.; Rodlert, M.; Bucaille, J.-L.; Grünbauer, H. J. M.; Månson, J.-A. E. *Polymer* **2005** 46, 6543-6553.
114. Hong, Y.; Coombs, S. J.; Cooper-White, J. J.; Mackay, M. E.; Hawker, C. J.; Malmström, E.; Rehnberg, N. *Polymer* **2000** 41, 7705-7713.
115. Nunez, C. M.; Chiou, B.-S.; Andrady, A. L.; Khan, S. A. *Macromolecules* **2000** 33, 1720-1726.
116. Marsalko, T. M.; Majoros, I.; Kennedy, J. P. *J. Macromol. Sci., Pure Appl. Chem.* **1997** A34, 775-792.
117. Thompson, D. S.; Markoski, L. J.; Moore, J. S.; Sendjarevic, I.; Lee, A.; McHugh, A. J. *Macromolecules* **2000** 33, 6412-6415.
118. Elrehim, M. A.; Voit, B.; Bruchmann, B.; Eichorn, K.-J.; Grundke, K.; Bellman, C. J. *Polym. Sci.: Part A: Polym. Chem.* **2005** 43, 3376-3393.
119. Ishida, Y.; Sun, A. C. F.; Jikei, M.; Kakimoto, M. *Macromolecules* **2000** 33, 2832-2838.
120. Chen, H.; Yin, J. *J. Polym. Sci.: Part A: Polym. Chem.* **2002** 40, 3804-3814.
121. Baek, J.-B.; Harris, F. W. *Macromolecules* **2005** 2005, 1131-1140.
122. Peng, H.; Lam, J. W. Y.; Tang, B. Z. *Polymer* **2005** 46, 5746-5751.
123. Powell, K. T.; Cheng, C.; Gudipati, C. S.; Wooley, K. L. *J. Mater. Chem.* **2005** 15, 5128-5135.
124. Abdelrehim, M.; Komber, H.; Langenwalter, J.; Voit, B.; Bruchmann, B. *J. Polym. Sci.: Part A: Polym. Chem.* **2004** 42, 3062-3081.
125. Wu, D.; Liu, Y.; Chen, L.; He, C.; Chung, T. S.; Goh, S. H. *Macromolecules* **2005** 38, 5519-5525.
126. Fossum, E.; Tan, L.-S. *Polymer* **2005** 46, 9686-9693.
127. Ungar, G.; Zeng, X.-B. *Chem. Rev.* **2001** 101, 4157-4188.
128. Sato, Y. *J. Appl. Polym. Sci.* **1981** 26, 27-39.
129. Jayakannan, M.; Ramakrishnan, S. *J. Polym. Sci.: Part A: Polym. Chem.* **2000** 38, 261-268.

130. DeSimone, J. M. *Science* **1995** 269, 1060-1061.
131. Mai, Y.; Zhou, Y.; Yan, D.; Hou, J. *New J. Phys.* **2005** 7, 1-9.
132. Magnusson, H.; Malmström, E.; Hult, A.; Johansson, M. *Polymer* **2002** 43, 301-306.
133. Trollsås, M.; Atthoff, B.; Claesson, H.; Hedrick, J. L. *Macromolecules* **1998** 31.
134. Schmaljohann, D.; Häußler, L.; Pötschke, P.; Voit, B. I.; Loontjens, T. J. A. *Macromol. Chem. Phys.* **2000** 201, 49-57.
135. Seo, Y.; Kim, J.; Kim, K. U.; Kim, Y. C. *Polymer* **2000** 41, 2639-2646.
136. Weng, W.; Chen, G.; Dajun, W. *Polymer* **2003** 44, 8119-8132.

Chapter 3: Synthesis and Characterization of Highly Branched Ionenenes Containing Poly(tetramethylene oxide)

(Fornof, A.R.; Mallakpour, S.; Park, T.; Long, T.E. *Polymer* **2006**, *to be submitted*)

3.1 Abstract

Linear and highly branched ionenes, which are defined as polyelectrolytes with quaternary amines in the main chain, were synthesized. A modified Menshutkin reaction enabled the synthesis of highly branched ionenes, where the soft segment consisted of well-defined poly(tetramethylene oxide) (PTMO) and the ionic sites were incorporated at the branch points. The highly branched ionenes comprised well-defined linear segments between branch points. The influence of branched ionic segments was investigated, and the influence of the distance between branch points was examined. Two PTMO precursors were prepared, 2,000 and 7,000 g/mol, which are below and above the critical molecular weight for entanglement (PTMO $M_c = 2,500$ g/mol). The thermal stability and transitions of the linear and highly branched ionenes were determined using TGA, DMA, and DSC. The TGA and DSC of the ionenes were similar regardless of macromolecular topology. However, the DMA indicated a significant difference in the temperature dependence of the storage modulus for the linear and highly branched ionenes, where branching significantly reduced the storage modulus after crystalline melting of the PTMO soft segment. While molecular weight was not

determined for these systems, the influence of branching on the tensile properties was determined and implied that branching in the ionic hard segment influenced symmetry and impeded ionic aggregation resulting in different mechanical performance.

Keywords: ionenes, branching, mechanical behavior, ionic aggregation

3.2 Introduction

Ionenes, which are macromolecules that contain quaternary ammonium salts in the main chain, are considered a subset of cationic polyelectrolytes. Our primary interest in ionenes stems from the numerous applications for microphase separated, elastomeric polycations. Applications for these elastomeric polycations range from gene transfection agents to ionically conductive elastomers.¹³³⁻¹³⁵ Ionenes serve as ideal models for polyelectrolytes due to various structural parameters, including counterion selection, diverse functional precursors, block, alternating, and random copolymerization.^{136, 137} The Menshutkin reaction¹³⁸, which involves quantitative reactions of primary alkyl dihalides and tertiary diamines, is the conventional approach for the synthesis of polymeric ionenes.¹³⁹⁻¹⁴¹ The ease of adjusting the distance between ionic sites through changing the molecular weight of the diamine and/or dihalide enables this subclass of ionomers as excellent models for fundamental investigations of charge density and counterion binding in biological applications and model polyelectrolytes.¹⁴²⁻¹⁴⁴ Most work on ionenes has focused on the synthesis and characterization of ionenes with linear topology.¹⁴⁵⁻¹⁴⁷ However, a few studies have focused on the synthesis and solution properties of star-shaped (3- and 4-arm), hyperbranched, and comb ionenes with wholly aliphatic soft segments.^{148, 149} For example, studies based on rotaxanes focused on structure-property relationships for this unique architecture.¹⁵⁰

Linear ionenes with well-defined distances between ionic sites display microphase separation.¹⁵¹ The well-defined, segmented, structure of ionenes, which leads to the microphase separated morphologies, differed from conventional random placement of ionic groups as pendant groups in ionomers.^{152, 153} Microphase separated ionenes are

attractive elastomeric materials due to high tensile strength (>30 MPa) and elongation (>1000%). However, ammonium based ionenes have interesting mechanical properties and ionic conductivity are also thermally unstable.¹⁵⁴⁻¹⁵⁶ Ionenes undergo depolymerization through dequaternization of the ammonium cation, also known as the Hofmann elimination.¹⁴¹ Ionenes can undergo a re-quaternization of the ammonium cation at elevated temperatures; however, the process is slow and frequently does not regenerate the original higher molecular weights prior to degradation.¹⁴¹ The proclivity for degradation through the Hoffmann reaction depends on the basicity of the counterion, but the lack of thermal stability precludes some ionenes from melt processing.¹⁵⁰ One earlier approach in order to improve the melt processibility included the incorporation of a plasticizer.¹⁵²

Branching significantly influences melt viscosity, which leads to improvements in melt processibility, in the absence of additives. Dendritic and hyperbranched polymers²⁸ are frequently described as rheological modifiers.^{10, 32} However, the high degree of branching in these polymers restricts entanglement and resulting mechanical properties are often inferior relative to linear analogs.³⁷ Our research group has described highly branched polymers, where linear units are incorporated between branch points, using an *oligomeric* A₂ plus a monomeric B₃.^{1, 7, 15, 16} The greater distance between branch points produces polymers with a high degree of branching, and acceptable mechanical properties.¹⁶ Also, these highly branched polymers offer reduced viscosities compared to linear analogs, which may improve both melt and solution processibility.¹⁵⁷

In this work, highly branched ionenes were synthesized via the *oligomeric* A₂ plus B₃ methodology. The effect of branching on the mechanical properties, rheological

behavior, and aggregation of ionic sites was explored. The incorporation of branching is proposed to influence the processibility of ionenes as well as elucidate the influence of branch points in the ionic segment on microphase separation through indirect techniques and mechanical performance.

3.3 Experimental

3.3.1 Materials

Chromatographic grade tetrahydrofuran (THF) was purchased from EMD Chemicals and distilled over sodium immediately prior to use. Irganox 1076 was obtained from Ciba Specialty Chemical Co. Trifluoromethanesulfonic anhydride (TFMSA), methyl 3-(dimethylamino) propionate, and 2,4,6-tris(bromomethyl)mesitylene (TBMM) were purchased from Aldrich and used without further purification. Dichloromethane (DCM), toluene, and hexanes were purchased from EMD Chemicals and used without further purification.

3.3.2 Synthesis of telechelic bis(dimethylamino) poly(tetramethylene oxide)

Synthesis of a 2,000 g/mol telechelic bis(dimethylamino) poly(tetramethylene oxide) (BAPTMO) oligomer involved the addition of TFMSA (3.38 mL, 0.02 mol) with a syringe to a solution of dry THF (10.00 g, 0.1389 mol) and DCM (10.00 g, 0.1177 mol) in a three-necked, round-bottomed, 250-mL flask in an ice bath. After 15 min, dry THF (30.00 g, 0.4167 mol) was added dropwise to the solution. Once the dry THF was completely added (approximately 15 min), the reaction was mechanically stirred for 90 min at 0 °C. Toluene (100 mL) was added to the reaction with excess methyl 3-

(dimethylamino) propionate (11.4 mL, 0.08 mol). The reaction was removed from the ice bath and continued for 30 min at room temperature with mechanical stirring. The solution was precipitated into hexanes to remove residual methyl 3-(dimethylamino) propionate, and hexanes were decanted. The reaction was poured into a 500-mL, round-bottomed flask with approximately 50 mL toluene and 100 mL 25 wt% aqueous NaOH solution. The reaction was refluxed for 30 min to remove residual acid and to convert the quaternary amine end groups to tertiary amines via a reverse Michael addition. The aqueous layer was discarded, and the toluene solution was dried over MgSO_4 and filtered. The solution was precipitated into hexanes to remove residual 2-ethyl acrylate, which is the byproduct of the reverse Michael addition. The BAPTMO product was dried under reduced pressure at 60 °C overnight to remove residual solvent. The BAPTMO in a solution of THF and isopropanol (3:1 vol:vol mixture) was titrated with 0.1 N HCl in isopropanol in order to determine the number average molecular weight.

3.3.3 Synthesis of highly branched ionenes

2,000 g/mol BAPTMO (4.7680 g, 2.384 mmol) was dissolved in dry THF at 15 wt%. TBMM (0.9516 g, 2.384 mmol) was dissolved in a two-necked, round-bottomed, 500-mL flask with dry THF to 3 wt%. The BAPTMO solution was slowly added dropwise to the TBMM solution under reflux conditions. The reaction proceeded for 1 h with magnetic stirring. At the end of the reaction, 0.02 g Irganox 1076 was added, and the solution was cast on a glass plate. The cast film was dried for 16 h at 25 °C and ambient pressure, and residual THF was removed under reduced pressure at 60 °C for 24 h.

3.3.4 Synthesis of linear ionenes

Linear ionenes were synthesized using 1,4-dibromo-*p*-xylene. For example, the 2,000 g/mol BAPTMO (4.3700 g, 2.2185 mmol) was added to a solution of dry THF and 2.5% excess 1,4-dibromo-*p*-xylene (0.5915 g, 2.241 mmol). The reaction proceeded under reflux until the magnetic stir bar was not able to rotate due to the high viscosity of the solution (approximately 1 h). The films were cast on glass slides, dried at 25 °C and ambient pressure for 16 h, and finally dried under reduced pressure at 60 °C for 24 h to ensure the removal of THF.

3.3.5 Characterization

The stress–strain behavior of the films was determined with mini dog-bone films (2.91 x 10 mm), where 10 mm is the gauge length, which were cut using a bench-top die. An Instron Model 4400 Universal Testing System and Series IX software were used for stress-strain experiments. A crosshead speed of 50 mm/min was used until failure, and load versus displacement was recorded. Three to five samples were measured and their results were averaged to determine modulus, yield strength, and strain-at-break for each composition. Hysteresis experiments were performed after the films were stretched to either 100 or 200% strain at a crosshead speed of 50 mm/min and then immediately returned to the initial position (0% strain) at the same rate. Dynamic mechanical analysis (DMA) was performed on a TA Instruments DMA Q800 in tension mode at 5 °C/min and 1 Hz. A Perkin-Elmer Pyris 1 cryogenic instrument was used for differential scanning calorimetry (DSC) at a heating rate of 10 °C/min under nitrogen. A Varian Unity 400 MHz NMR spectrometer was employed at 25 °C using *d*-chloroform.

3.3 Results and Discussion

The highly branched topology provided an opportunity for fundamentally probing the effect of branching on the structure and mechanical performance of ionenes. Highly branched ionenes were synthesized via a modified Menschutkin reaction, and dihalides were replaced with trifunctional reactive halides. Tris(bromomethyl)mesitylene (TBMM) and bis(dimethylamino) poly(tetramethylene oxide) (BAPTMO) were used in a 1:1 molar stoichiometry. BAPTMO was synthesized from the living cationic polymerization of tetrahydrofuran (THF) (Scheme 3.1). Trifluoromethanesulfonic anhydride was used as the initiator to achieve a difunctional PTMO. The molecular weight of PTMO was controlled through adjustment of the monomer to initiator ratio, which is a typical strategy for control of molecular weight for living polymerizations. The living cationic PTMO was endcapped with methyl 3-(dimethylamino) propionate instead of dimethyl amine, which was used previously,¹⁴¹ to avoid further alkylation of the amine during the endcapping process. Upon completion of the reaction of living PTMO with methyl 3-(dimethylamino) propionate, the quaternary amine was converted to a tertiary amine through a reverse Michael addition. The products of the reverse Michael addition were the BAPTMO and methyl acrylate. The methyl acrylate was efficiently removed during precipitation and BAPTMO was subsequently used as the *oligomeric* A₂ in the synthesis of highly branched ionenes. Two molecular weights of BAPTMO were synthesized (approximately 2,000 and 7,000 g/mol), and the molecular weights calculated from integration of ¹H NMR spectra agreed well with titration of the amine endgroups (Table 3.1). BAPTMO (A₂) was added dropwise to a dilute solution of

